

AD-A095 030

PRATT AND WHITNEY AIRCRAFT GROUP WEST PALM BEACH FL 6--ETC F/8 14/2  
SPIN PIT APPLICATION OF IMAGE DEROTATED HOLOGRAPHIC INTERFEROME--ETC(U)  
SEP 80 J L BEARDEN, J F CLARADY F33615-79-C-2071

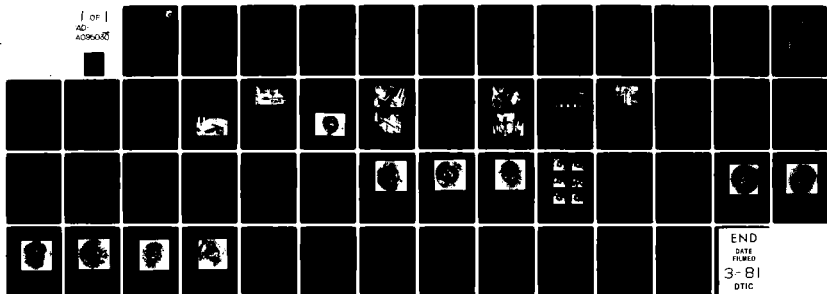
UNCLASSIFIED

PWA-FR-13041

AFWAL-TR-80-2083

ML

[ of ]  
AD  
A096000



END  
DATE  
FILMED  
3-81  
DTIC

AFWAL-TR-80-2083

LEVEL

2



# SPIN PIT APPLICATION OF IMAGE DEROTATED HOLOGRAPHIC INTERFEROMETRY

AD A095030

J. L. Bearden and J. F. Clarady  
United Technologies Corporation  
Pratt & Whitney Aircraft Group  
Government Products Division  
P.O. 2691, West Palm Beach, Florida 33402



September 1980

Technical Report AFWAL-TR-80-2083  
Final Report for Period 22 October 1979 - 15 September 1980

Approved for Public Release, Distribution Unlimited

AERO-PROPULSION LABORATORY  
AIR FORCE WRIGHT AERONAUTICAL LABORATORIES  
AIR FORCE SYSTEMS COMMAND  
WRIGHT-PATTERSON AIR FORCE BASE, OHIO 45433


81 2 17 040

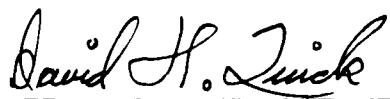
NOTICE

When Government drawings, specifications, or other data are used for any purpose other than in connection with a definitely related Government procurement operation, the United States Government thereby incurs no responsibility nor any obligation whatsoever; and the fact that the government may have formulated, furnished, or in any way supplied the said drawings, specifications, or other data, is not to be regarded by implication or otherwise as in any manner licensing the holder or any other person or corporation, or conveying any rights or permission to manufacture use, or sell any patented invention that may in any way be related thereto.

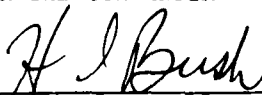
This report has been reviewed by the Office of Public Affairs (ASD/PA) and is releasable to the National Technical Information Service (NTIS). At NTIS, it will be available to the general public, including foreign nations.

This technical report has been reviewed and is approved for publication.

  
\_\_\_\_\_  
JAMES C. MACBAIN  
Project Engineer

  
\_\_\_\_\_  
DAVID H. QUICK, Lt Col, USAF  
Chief, Components Branch  
Turbine Engine Division

FOR THE COMMANDER

  
\_\_\_\_\_  
H. I. BUSH  
Acting Director  
Turbine Engine Division

"If your address has changed, if you wish to be removed from our mailing list, or if the addressee is no longer employed by your organization please notify AFWAL/POTC, W-PAFB, OH 45433 to help us maintain a current mailing list".

Copies of this report should not be returned unless return is required by security considerations, contractual obligations, or notice on a specific document.

SECURITY CLASSIFICATION OF THIS PAGE (When Data Entered)

REPORT DOCUMENTATION PAGE		READ INSTRUCTIONS BEFORE COMPLETING FORM
1. Report Number AFWAL-TR-80-2083	2. Govt Accession No. AD-H095-030	3. Recipient's Catalog Number
4. Title (and Subtitle) SPIN PIT APPLICATION OF IMAGE DEROTATED HOLOGRAPHIC INTERFEROMETRY		5. Type of Report & Period Covered Final Report 22 October 1979 - 15 September 1980
7. Author(s) J. L. Bearden J. F. Clarady		6. Performing Org. Report Number FR-13041
9. Performing Organization Name and Address United Technologies Corporation Pratt & Whitney Aircraft Group Government Products Division P.O. Box 2691, West Palm Beach, FL 33402		8. Contract or Grant Number(s) F33615-79-C-2071 new
11. Controlling Office Name and Address Aero-Propulsion Laboratory Air Force Wright Aeronautical Laboratories, AFSC Wright-Patterson AFB, Ohio 45433		10. Program Element, Project, Task Area & Work Unit Numbers 646100, 3066/306612, 30661261
14. Monitoring Agency Name & Address (if different from Controlling Office)		12. Report Date September 1980 17 12
		13. Number of Pages 49
16. Distribution Statement (of this Report) Approved for Public Release, Distribution Unlimited		15. Security Class. (of this report) Unclassified
		15a. Declassification/Downgrading Schedule
17. Distribution Statement (of the abstract entered in Block 20, if different from Report)		
18. Supplementary Notes		
19. Key Words (Continue on reverse side if necessary and identify by block number) Image Derotated Holographic Interferometry Spin Test Facility Bladed Disk Assembly Electromagnetic Excitation		
20. Abstract (Continue on reverse side if necessary and identify by block number) This report describes the results of a program in which an experimental technique for image derotated holographic interferometry was developed to investigate the resonant response of a gas turbine engine bladed-disk assembly under controlled laboratory conditions of rotation and vibratory excitation. Image derotated holograms were taken for several modes of vibration of a rotating bladed disk at speeds up to 7,500 rpm in a laboratory spin test facility.		

DD FORM 1473 1 JAN 73

EDITION OF 1 NOV 65 IS OBSOLETE

SECURITY CLASSIFICATION OF THIS PAGE (When Data Entered)

## FOREWORD

This report covers the work performed under AFWAL/POTC Contract F33615-79-C-2071 from 22 October 1979 to 15 July 1980 with Dr. James C. MacBain as Project Manager. This program was conducted in the Materials Engineering and Technology Laboratories of Pratt & Whitney Aircraft Group, Government Products Division, West Palm Beach, Florida under the direction of Mr. J. L. Bearden, Program Manager, and Mr. J. F. Clarady, Principal Investigator. The program element, project, task area and work unit numbers are 646100, 3066, 306612, 30661261, respectively.

The following personnel are acknowledged for technical effort which contributed significantly to this program:

Mr. J. Weber	—	Rotating Structures
Mr. J. Schratt	—	Rotating Structures
Mr. R. Cummins	—	Optical/Special Analysis
Mr. W. Chartier	—	Optical/Special Analysis
Mr. B. Benedict	—	Modal Analysis

Accession For	
NTIS GRA&I	<input checked="" type="checkbox"/>
DTIC TAB	<input type="checkbox"/>
Unannounced	<input type="checkbox"/>
Justification	<input type="checkbox"/>
By	
Distribution/	
Availability Codes	
Avail and/or	
Dist	
A	

## TABLE OF CONTENTS

<i>Section</i>		<i>Page</i>
I	INTRODUCTION.....	1
II	TEST STRUCTURE.....	2
III	TEST FACILITIES.....	7
	1. Spin Test Facility.....	7
	2. Image Derotator System.....	11
	3. Strain Gage Instrumentation.....	13
	4. Electromagnet Excitation System.....	14
IV	HOLOGRAPHIC INTERFEROMETRY OF A ROTATING STRUCTURE	17
	1. Test Concept.....	17
	2. Resonant Response of a Rotating Disk.....	18
	3. Excitation Method.....	20
	4. Experimental Technique.....	20
	5. Data Analysis.....	26
V	CONCLUSIONS AND RECOMMENDATIONS.....	41
	REFERENCES.....	42

## LIST OF ILLUSTRATIONS

<i>Figure</i>		<i>Page</i>
1	J52 2nd-Stage Compressor Bladed-Disk Showing Magnetic Ring Used During ac Electromagnetic Excitation.....	3
2	J52 2nd-Stage Compressor Bladed-Disk Mounted in the Spin Test Facility Showing Spin Tooling and Electromagnets.....	3
3	J52 2nd-Stage Compressor Bladed-Disk, Magnetic Ring, and Spin Tooling Assembly Used in Image Derotated Holographic Interferometry.....	4
4	J52 2nd-Stage Compressor Blade Showing Location and Orientation of Strain Gages.....	5
5	New Spin Test Facility.....	7
6	Spin Test Facility With Lid Raised To Show Bladed-Disk and Top of Vacuum Chamber.....	8
7	New Spin Test Facility Used for Present Program Development of Image Derotated Holography.....	8
8	Old Spin Test Facility Used for Feasibility Study of Image Derotated Holography.....	9
9	Image Derotated Hologram of F100 2nd-Stage Turbine Bladed-Disk Taken During Feasibility Study Showing Bias Fringe Pattern Resulting from Plexiglass Cover.....	9
10	Optics Room of New Spin Test Facility.....	10
11	Control Room of New Spin Test Facility Showing Laser, Electromagnet and Derotator Control Instrumentation as Well as Strain Gage Monitoring and Recording Instrumentation.....	10
12	Experimental Setup for Image Derotated Holographic Interferometry in the Spin Test Facility.....	11
13	Optics Table Setup for Image Derotated Holographic Interferometry.....	12
14	Image Derotator With Objective, Field and Copy Lenses.....	12
15	Image Derotator Control Unit.....	13
16	Top of Spin Test Facility Showing Slipring, Code Wheel and Optical Sensor	14
17	Strain Gage Data Acquisition and Analysis Instrumentation.....	15
18	The ac Electromagnetic Excitation System.....	15
19	Typical Mode Shapes of 2N and 2N-1S Modes of Vibration of a Circular Disk.....	18

## LIST OF ILLUSTRATIONS (Continued)

<i>Figure</i>		<i>Page</i>
20	Excitation Frequencies for a Rotating Disk in the $n^{\text{th}}$ Mode of Vibration With a Response Frequency of $P_n$ .....	19
21	Experimental Results With dc Magnetic Excitation Taken from the Feasibility Study of the F100 2nd-Stage Turbine Disk.....	21
22	Procedure for Optical Alignment of Axes of Rotation for the Bladed-Disk and Image Derotator: (a) Adjustment of 45-deg Mirror and Translation of Double-Folding Mirrors To Center the Two Axes of Rotation, and (b) Tilting of the Upper Mirror in the Double-Folding Mirror Assembly To Make the Two Axes Coincidental.....	22
23	Image Derotated Double Exposure Hologram of J52 2nd-Stage Compressor Bladed-Disk Rotating at 9000 rpm With No Vibratory Excitation (Pulse Separation Was $40\mu$ sec).....	24
24	Image Derotated Double Exposure Hologram Showing Misalignment Bias Fringe Pattern (Pulse Separation Was $40\mu$ sec).....	25
25	Image Derotated Double Exposure Hologram of J52 2nd-Stage Compressor Bladed-Disk Showing Contour Fringes Resulting from Multimoding of Double Pulsed Ruby Laser.....	26
26	Reconstructed Time Average Holograms of Nonrotating J52 2nd-Stage Compressor Bladed-Disk.....	27
27	Excitation and Response Frequencies as a Function of Bladed-Disk Rotation Speed for the 2N, 1N-1S, 2N-1S and 3N-1S Modes of Vibration.....	29
28	Image Derotated Double Exposure Hologram of the 3N-1S Mode of Vibration of the J52 2nd-Stage Compressor Bladed-Disk Rotation at 7500 rpm (the Excitation Frequency Was 300 Hz and the Response Frequency Was 670 Hz).....	30
29	Image Derotated Double Exposure Hologram of the 3N-1S Mode of Vibration of the J52 2nd-Stage Compressor Bladed-Disk Rotating at 7500 rpm (the Excitation Frequency Was 296 Hz and the Response Frequency Was 674 Hz).....	31
30	Image Derotated Double Exposure Hologram of the 3N-1S Mode of Vibration of the J52 2nd-Stage Compressor Bladed-Disk Rotating at 7000 rpm (the Excitation Frequency Was 310 Hz and the Response Frequency Was 657 Hz).....	32
31	Image Derotated Double Exposure Hologram of the 1N-1S Mode of Vibration of the J52 2nd-Stage Compressor Bladed-Disk Rotating at 7500 rpm (the Excitation Frequency Was 550 Hz and the Response Frequency Was 425 Hz).....	33



**LIST OF ILLUSTRATIONS (Continued)**

<i>Figure</i>		<i>Page</i>
32	Image Derotated Double Exposure Hologram of the 1N-1S Mode of Vibration of the J52 2nd-Stage Compressor Bladed-Disk Rotating at 7500 rpm (the Excitation Frequency) Was 544 Hz and the Response Frequency Was 422 Hz).....	34
33	Image Derotated Double Exposure Hologram of the 2N Mode of Vibration of the J52 2nd-Stage Compressor Bladed-Disk Rotating at 7500 rpm (the Excitation Frequency Was 620 Hz and the Response Frequency Was 370 Hz).....	35
34	Spectral Response Curves for the Indicated Strain Gages Mounted on a J52 2nd-Stage Compressor Bladed-Disk Rotating at 7000 rpm and Excited in the 2N Mode of Vibration With an Excitation Frequency of 592 Hz.....	36
35	Spectral Response Curves for the Indicated Strain Gages Mounted on a J52 2nd-Stage Compressor Bladed-Disk Rotating at 7000 rpm and Excited in the 1N-1S Mode of Vibration With an Excitation Frequency of 538 Hz.....	37
36	Spectral Response Curves for the Indicated Strain Gages Mounted on a J52 2nd-Stage Compressor Bladed-Disk Rotating at 7000 rpm and Excited in the 2N-1S Mode of Vibration With an Excitation Frequency of 334 Hz.....	38
37	Spectral Response Curves for the Indicated Strain Gages Mounted on a J52 2nd-Stage Compressor Bladed-Disk Rotating at 7000 rpm and Excited in the 2N-1S Mode of Vibration With an Excitation Frequency of 794 Hz.....	39
38	Spectral Response Curves for the Indicated Strain Gages Mounted on a J52 2nd-Stage Compressor Bladed-Disk Rotating at 7000 rpm and Excited in the 3N-1S Mode of Vibration With an Excitation Frequency of 310 Hz.....	40

## SUMMARY

This program developed an experimental technique of image derotated holographic interferometry to investigate the resonant response of a gas turbine engine bladed-disk under controlled laboratory conditions of rotation and vibratory excitation. Image derotated holograms were taken of several modes of vibration of a rotating bladed-disk at rotational speeds of 7500 rpm in a laboratory spin test facility.

## SECTION I

### INTRODUCTION

The objective of this program was to develop an experimental technique of image derotated holographic interferometry in order to study the resonant behavior of gas turbine engine bladed-disks under controlled conditions of rotation and vibratory excitation. This program was intended to continue the development initiated in a feasibility study funded under Air Force Aero-Propulsion Laboratory (AFAPL) Contract F33615-77-C-2093.

The ever-increasing need for high-performance fighter aircraft, and the subsequent requirement for gas turbine engines of higher thrust-to-weight ratio has placed increasing emphasis on the development of improved vibration analysis techniques to more completely define the dynamic response of these high-technology engines. Of particular significance to the development of advanced gas turbine engines is the improved understanding of the vibratory response of the engines' rotating structures, such as the fan, compressor, and turbine bladed-disks. Current analysis of these rotating structures depends on laboratory testing, such as strain or holographic analysis or on instrumented engine tests. Both of these methods have significant disadvantages. Laboratory tests require that a structure normally rotating during engine operation be studied under nonrotating conditions. Instrumented engine tests are extremely expensive and time consuming, and the results are often clouded by the complexities of testing an entire engine and the quality of the data obtained.

Therefore, the development of an experimental technique that would provide analysis of the dynamic response of an individual bladed-disk in a controllable laboratory environment of rotational speed and vibratory excitation would be advantageous. It is the goal of this program to develop such a technique by combining the optical image derotator system developed by K. Stetson at the United Technologies Research Center, under an Air Force contract (Reference 1), with the method developed at Pratt & Whitney Aircraft Group, Government Products Division (P&WA/GPD) for inducing a controlled vibratory excitation into a rotating bladed-disk. This technique would provide a method to accomplish holographic analysis of a rotating, fully bladed-disk to characterize the effects of rotation on the dynamic response of the bladed disk.

A feasibility study of the spin pit application of image derotated holographic interferometry was conducted under AFAPL Contract F33615-77-C-2093 (Reference 2). Although this earlier program did prove the feasibility of the basic technique, there were several unsolved problems remaining. This report details the improvements and advancements in the technique accomplished under this program.

## SECTION II

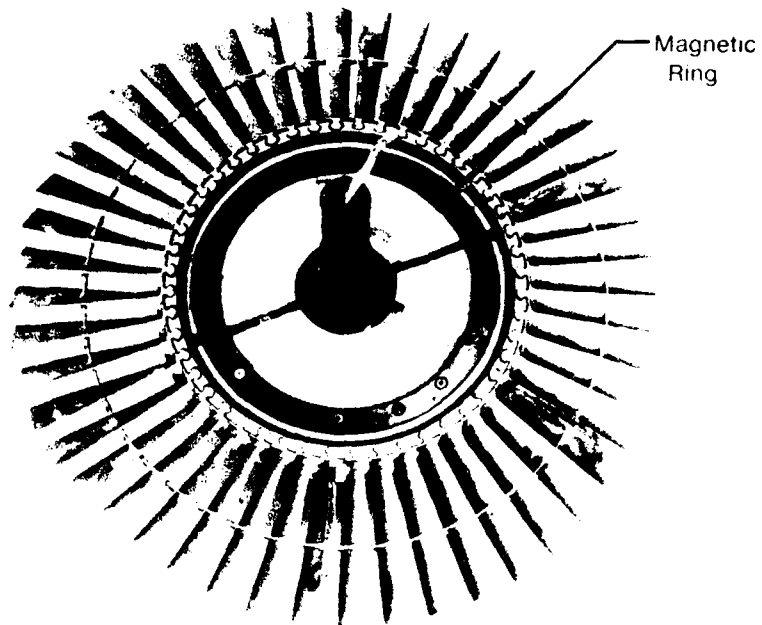
### TEST STRUCTURE

The test structure selected for this program was a J52 2nd-stage compressor bladed-disk assembly consisting of the disk and 48 shrouded compressor blades (Figure 1). The decision was made to change the test structure from the F100 2nd-stage turbine bladed-disk, used during the feasibility study, since the turbine disk proved to be extremely rigid, and a higher vibratory response could be induced in a more flexible structure. The selection of the J52 compressor bladed-disk was based on several factors which were: that the parts were available, the spin tooling was already fabricated saving considerable time and money, and the size of the structure was easily illuminated since it has a 28-in. diameter.

The blade root attachments were coated with W. T. Bean, Inc., epoxy-type room temperature cement shimmed with a 0.010 to 0.015-in.-thick steel shim and driven into the disk. Shims were also epoxied to the contact surface of each blade airfoil shroud in a way that prevented the shims from being thrown out during the rotating analysis but still allowing the shrouds to move relative to one another. This static loading of the blade roots and shrouds was to provide stiffness during the nonrotating holographic analysis and to assure adequate shroud loading during the rotating analysis in the absence of the aerodynamic load normally present on the blades during engine operation.

Spin tooling required for spin pit testing was assembled to the bladed-disk test structure, as shown in Figures 2 and 3, and consisted of a dishpan and spin arbor. All tests, including the nonrotating holographic analysis, were accomplished with the spin tooling attached to assure test structure uniformity. A magnetic ring used in conjunction with nonrotating electromagnets to provide vibratory excitation of the test structure was also attached to the disk during all tests. This ring was initially a stepped configuration with four raised lugs 90 deg apart. It was used for dc electromagnet excitation of the test structure early in the test program, and is described in detail later in Section IV. Subsequently, this ring was replaced by a continuous nonstepped ring (Figure 1) which, in conjunction with a nonrotating ac electromagnet, provided sinusoidal excitation to the rotating test structure.

Six blades, equally spaced in the disk, were instrumented with four strain gages, as shown in Figure 4. Gages were located based on the results of nonrotating holographic analysis and knowledge of the normal high-stress locations of shrouded blades. Strain gages were originally installed using 250°F limited epoxy. This temperature epoxy proved to be of low durability due to unexpected test structure temperatures resulting from induction heating of the test structure through the interaction of the electromagnets and the magnetic ring. Subsequently, the blades had to be reinstrumented using a higher temperature epoxy. Due to this heating of the bladed-disk, two thermocouples were mounted on the disk adjacent to the magnetic ring to monitor the temperature of the structure. This assured that the temperature stayed below the limitation of the strain gages. The strain gages and thermocouples were routed across the disk and dish pan and up the center of the spin arbor and drive shaft to a slipring mounted on the top of the drive turbine. A retroreflective paint was applied to the bladed-disk to provide a brighter image during the rotating holographic analysis.



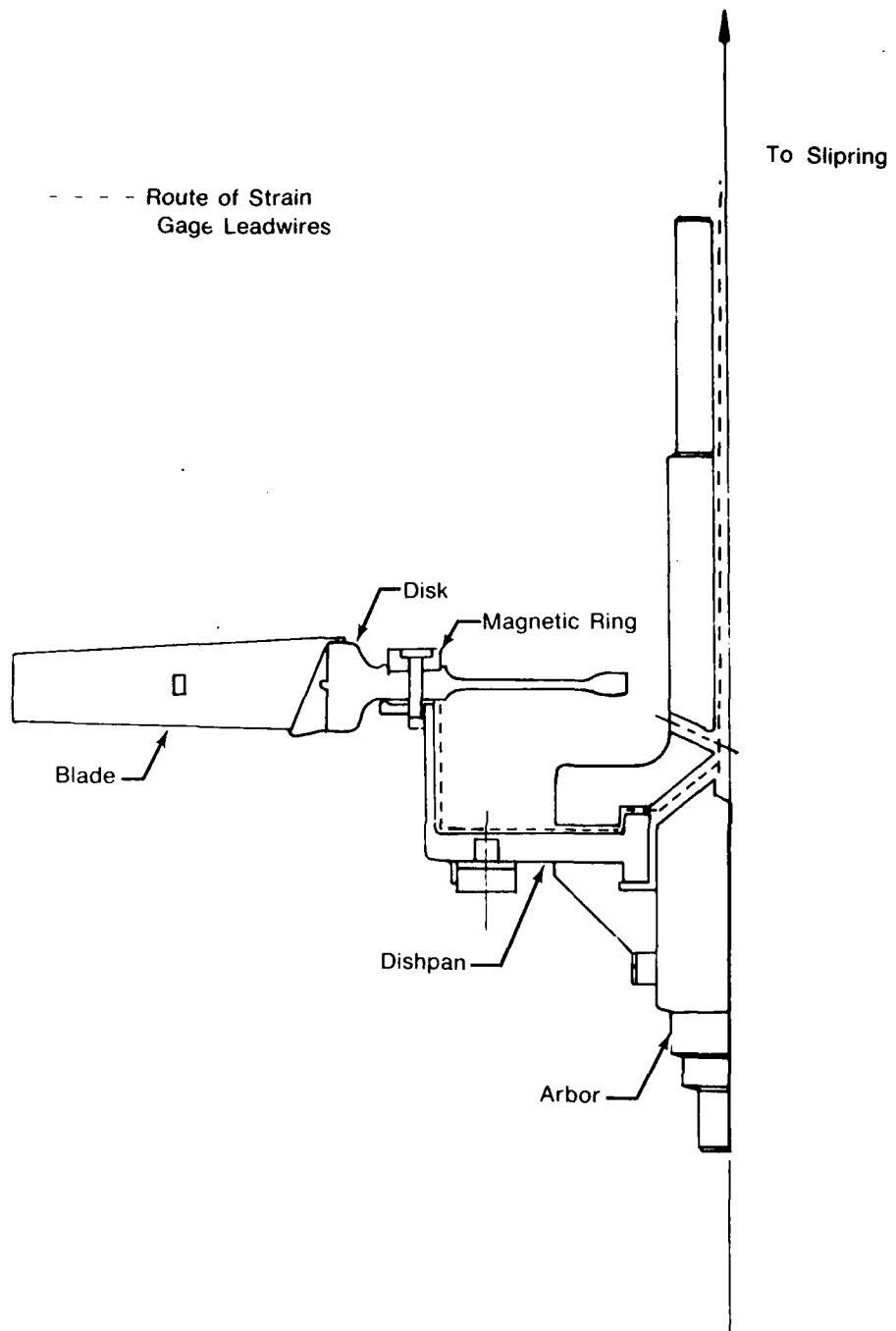
FE 191118 A

*Figure 1. J52 2nd-Stage Compressor Bladed-Disk Showing Magnetic Ring Used During ac Electromagnetic Excitation*



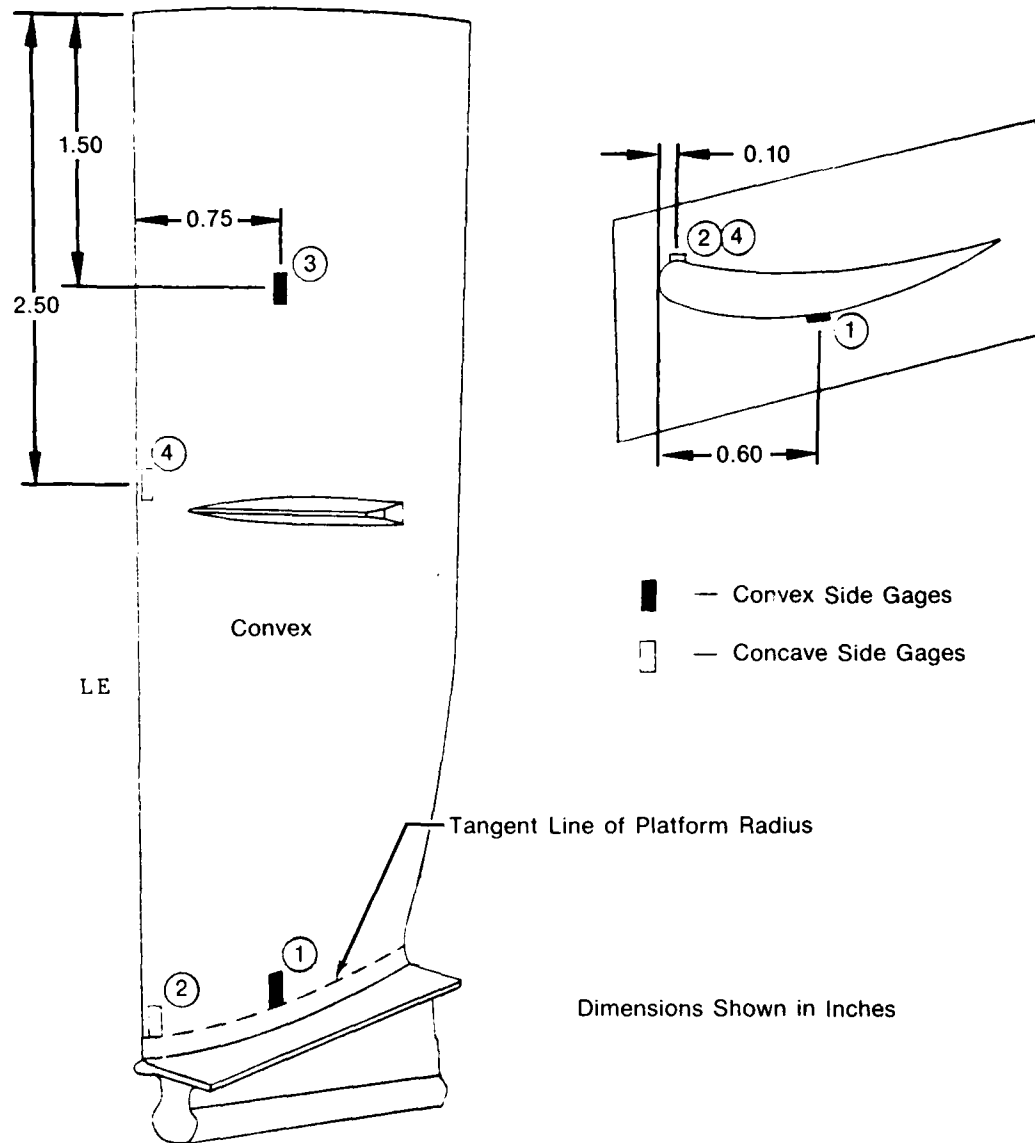
FE 185457A

*Figure 2. J52 2nd-Stage Compressor Bladed-Disk Mounted in the Spin Test Facility Showing Spin Tooling and Electromagnets*



FD 204177

*Figure 3. J52 2nd-Stage Compressor Bladed-Disk, Magnetic Ring, and Spin Tooling Assembly Used in Image Derotated Holographic Interferometry.*



FD 204178

Figure 4. J52 2nd-Stage Compressor Blade Showing Location and Orientation of Strain Gages

After the test structure was completely assembled, it was dynamically balanced on a low speed balance machine used to balance gas turbine engine bladed-disks prior to engine installation. Although the structure was balanced to 0.02 oz-in. or less, well within normal tolerances, it did not always spin stable in the spin pit, requiring several rebalances before a satisfactory spin was achieved. This inconsistency between the balance machine and the spin pit is probably attributable to the slow speed at which the bladed-disk was balanced (500 to 1000 rpm) compared to the high speeds encountered in the spin pit (7000 to 10,000 rpm). When the bladed-disk was balanced, it was supported on either side of the disk, but in the spin pit there is only one point of support 33 in. from the disk. Therefore, the spin pit arrangement is much more sensitive to test structure imbalance.



**SECTION III**  
**TEST FACILITIES**

**1. SPIN TEST FACILITY**

Image derotated holographic interferometry was conducted on the test structure at the Pratt & Whitney Aircraft Group, Government Products Division's (P&WA/GPD) new spin test facility (Figures 5 and 6). The test structure was rotated by a 14-in. air drive turbine through a vertical drive shaft that descends through the lid of the spin pit and attaches to the spin arbor (Figure 7). The electromagnets are attached to the lid and positioned in close proximity (typically 0.050 in.) to the magnetic ring on the bladed-disk. The large 45-deg mirror used to direct the object beam to the bladed-disk is located beneath the test structure on a specially constructed mount that uses hydraulic actuators to provide rotation and tilt angle adjustment of the mirror from outside the pit. The bladed-disk, magnets, and mirror are all enclosed in a large vacuum chamber that includes a tunnel through the wall of the spin pit, terminating in an optical quality glass window.

This spin test facility incorporates several improvements over the older facility in which the initial feasibility study was conducted (Figure 8). Most significant was the enlargement of the vacuum chamber which eliminated the plexiglass cover that induced a large bias fringe pattern on the holograms, as shown in Figure 9. The mount for the large 45-deg mirror that permits adjustment of the mirror from outside of the spin pit has greatly facilitated the alignment of the derotator optical system. The new facility also includes an optics room (Figure 10) that houses the optical system and lasers in an environmentally controlled area, and a control room for the derotator and laser controls as well as the strain gage conditioning and recording equipment (Figure 11).

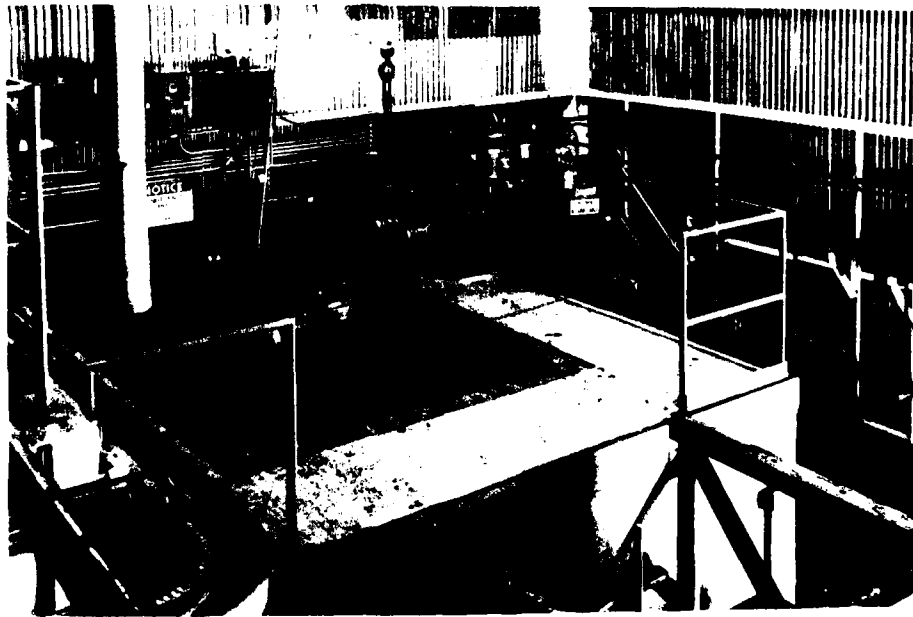


*Figure 5. New Spin Test Facility*

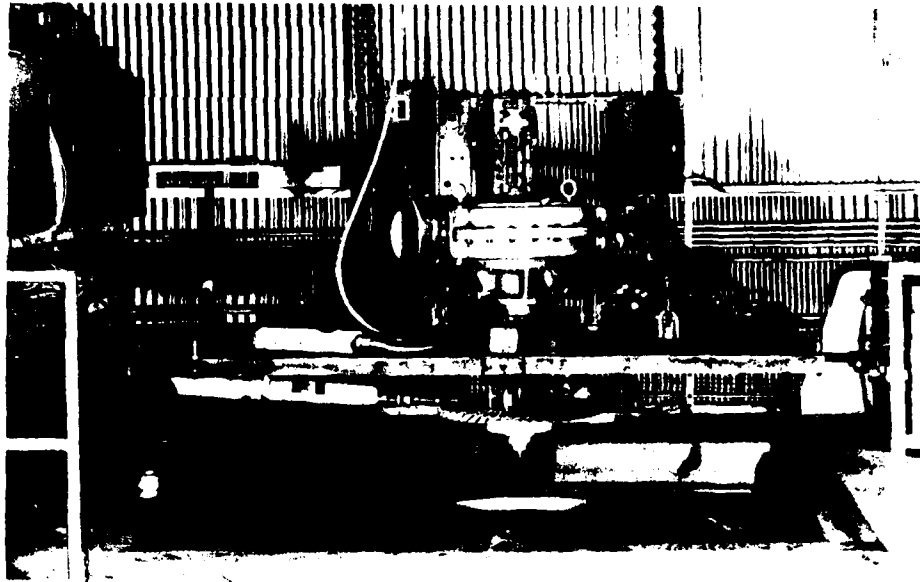
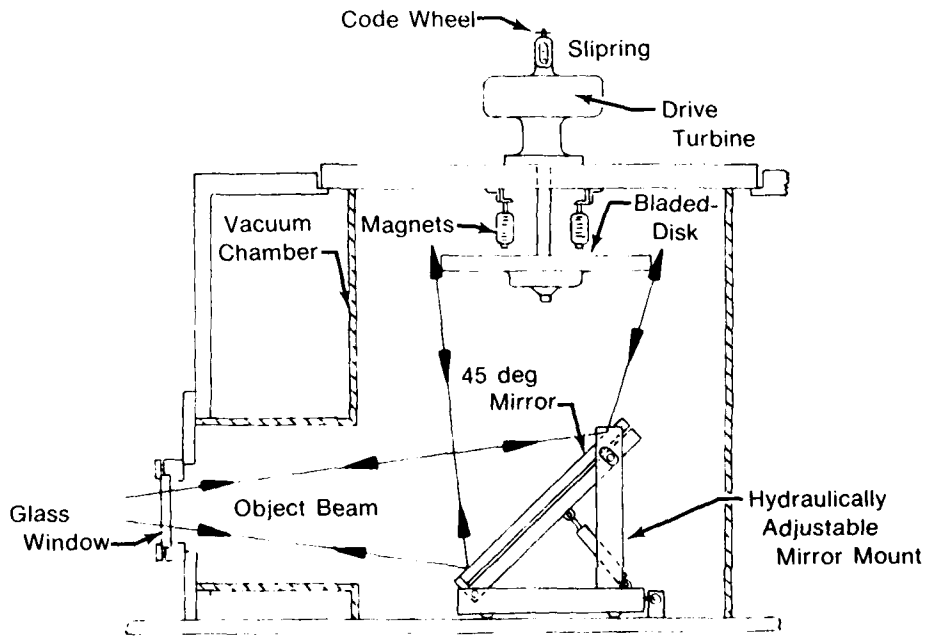


Figure 6. Spin Test Facility With Lid Raised To Show Bladed-Disk and Top of Vacuum Chamber



FD 204179

Figure 7. New Spin Test Facility Used for Present Program Development of Image Derotated Holography

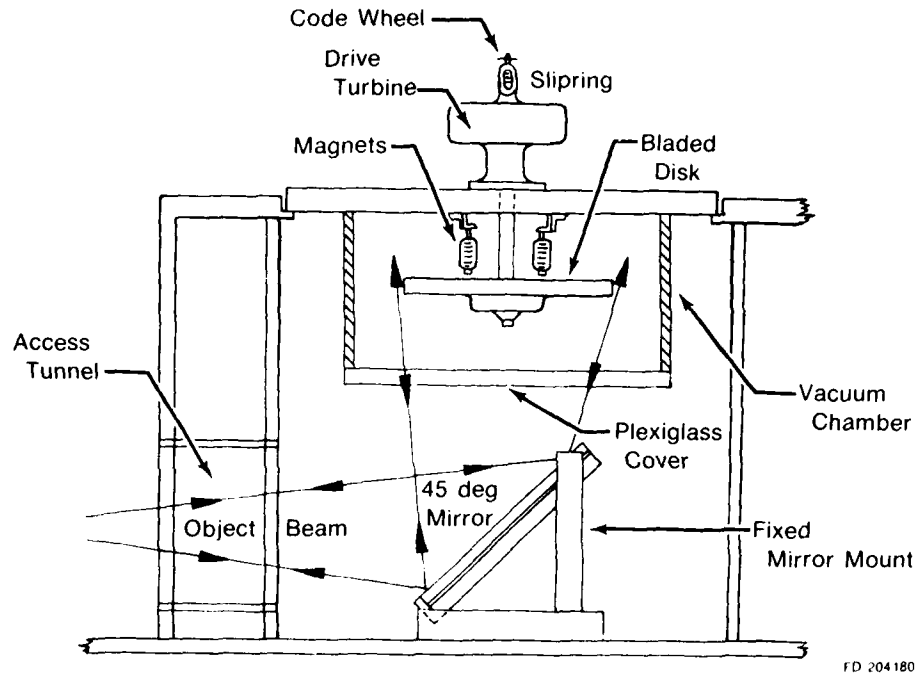


Figure 8. Old Spin Test Facility Used for Feasibility Study of Image De-rotated Holography

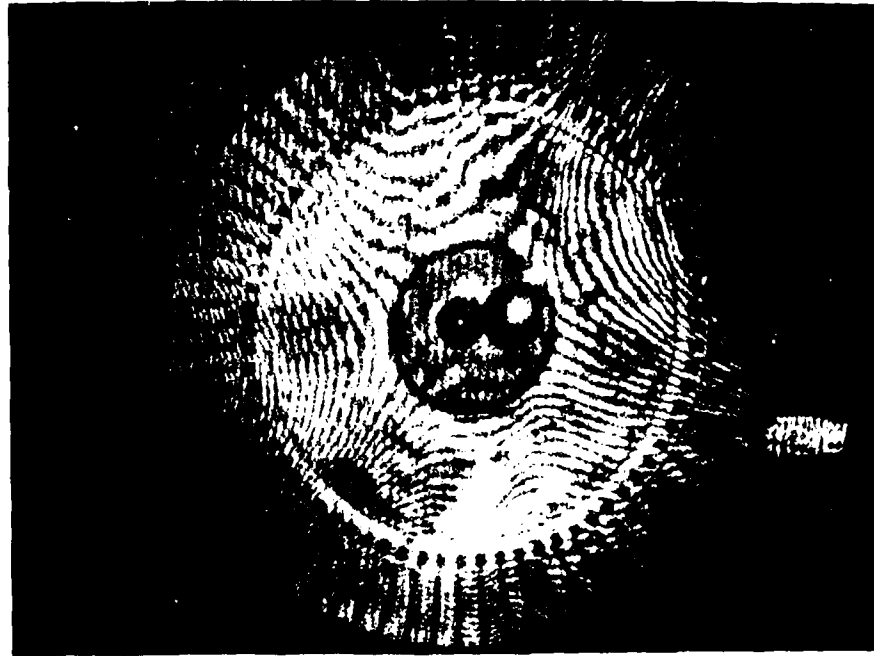
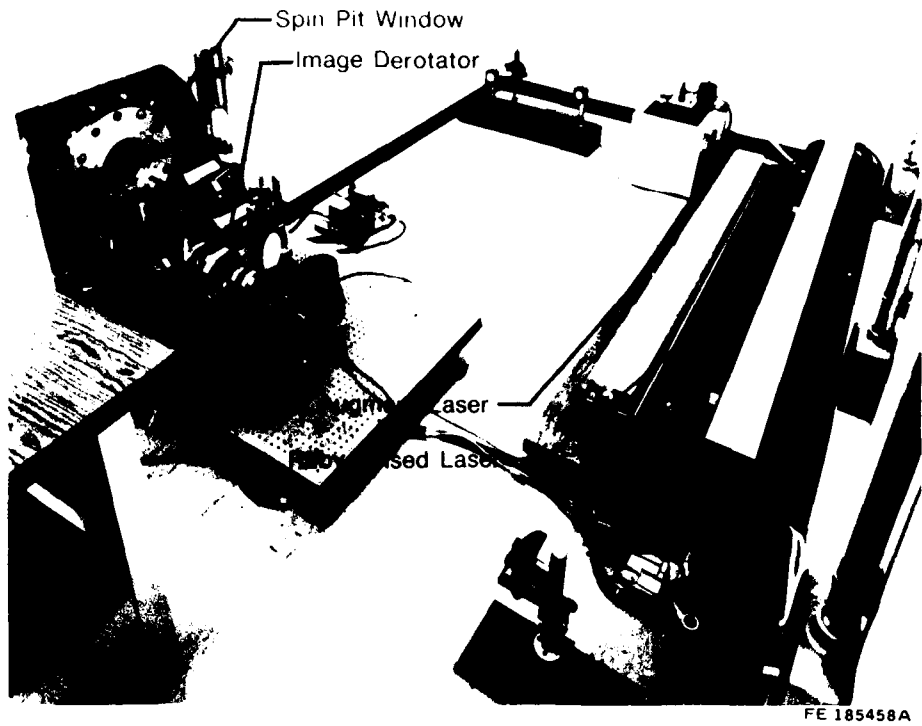
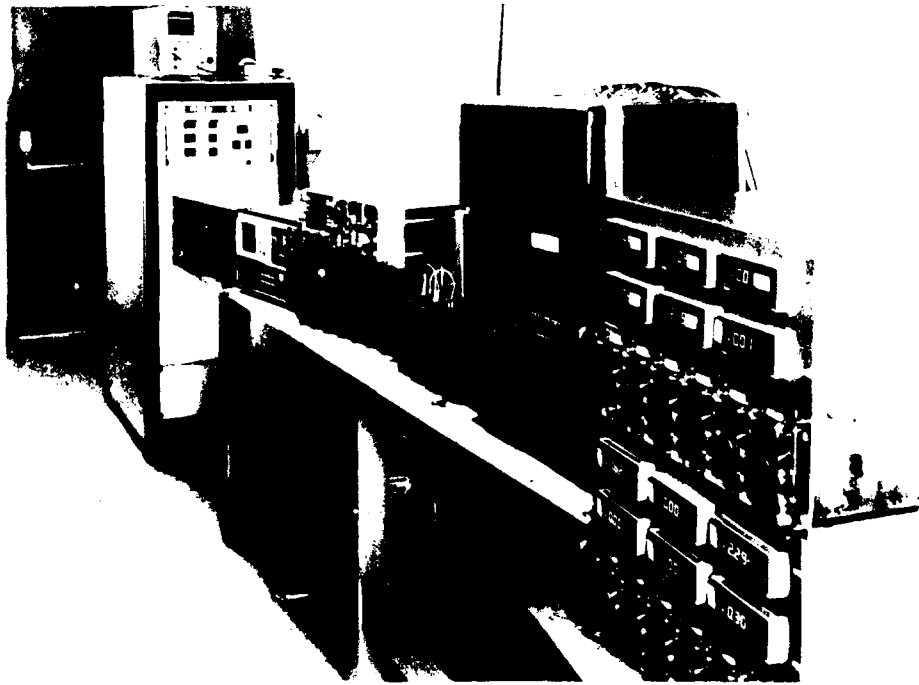


Figure 9. Image Derotated Hologram of F100 2nd-Stage Turbine Bladed-Disk Taken During Feasibility Study Showing Bias Fringe Pattern Resulting from Plexiglass Cover



FE 185458A

Figure 10. Optics Room of New Spin Test Facility



FE 191059A

Figure 11. Control Room of New Spin Test Facility Showing Laser, Electromagnet and Derotator Control Instrumentation as Well as Strain Gage Monitoring and Recording Instrumentation

## 2. IMAGE DEROTATOR SYSTEM

The image derotator optical and electronic systems consist of image derotator and associated optics and electronics, an Apollo Laser, Inc., Q-switched double-pulsed ruby laser, and a Spectra Physics, Inc., 50 mw helium-neon laser, as shown in Figures 12 through 15. The pulsed laser beam, after reflecting from mirrors  $M_1$  and  $M_2$ , passes through lens  $L_1$  to expand the beam and through a 50/50 beam splitter. The object beam reflected from mirror  $M_3$ , which in reality is a double-folding mirror assembly, is directed through the glass window and tunnel to the large 45-deg mirror at the bottom of the spin pit, which directs the object beam upwards to illuminate the rotating bladed-disk. Light reflected from the bladed-disk returns along the same path to the beam splitter, where it is reflected through the objective lens ( $L_2$ ), the image derotator, the field and copy lenses ( $L_3$  and  $L_4$ ), and finally to the film transport. The reference beam travels through a mirror system ( $M_4$  through  $M_6$ ) intended to make a path length equivalent to that of the object beam and to direct it to the film transport. The reference beam is detected by a photo diode.

The image derotator constructed at the United Technologies Research Center consists of a folded Abbe' prism mounted in a hollow shaft air bearing that is turned by a brushless dc torque motor. The speed of the derotator is controlled by a closed-loop system, including the dc motor, the derotator control unit (Figure 15), and two speed detector units consisting of a code wheel and optical sensor, one mounted on the derotator and the other on the end of the drive shaft on top of the slipring (Figure 16). The control unit compares the signals from the two speed detectors and then adjusts the current to the dc torque motor to lock on the derotator to precisely half the speed of the bladed-disk. The control unit must also maintain a constant rotational phase relationship between the derotator and the bladed-disk.

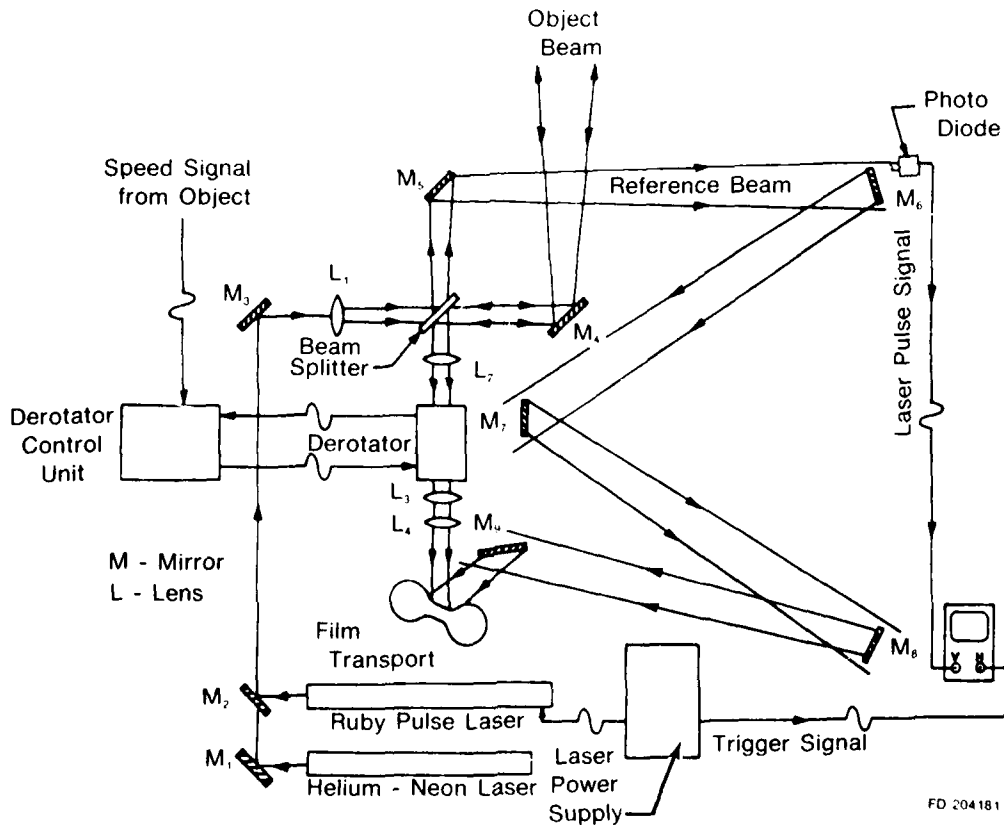
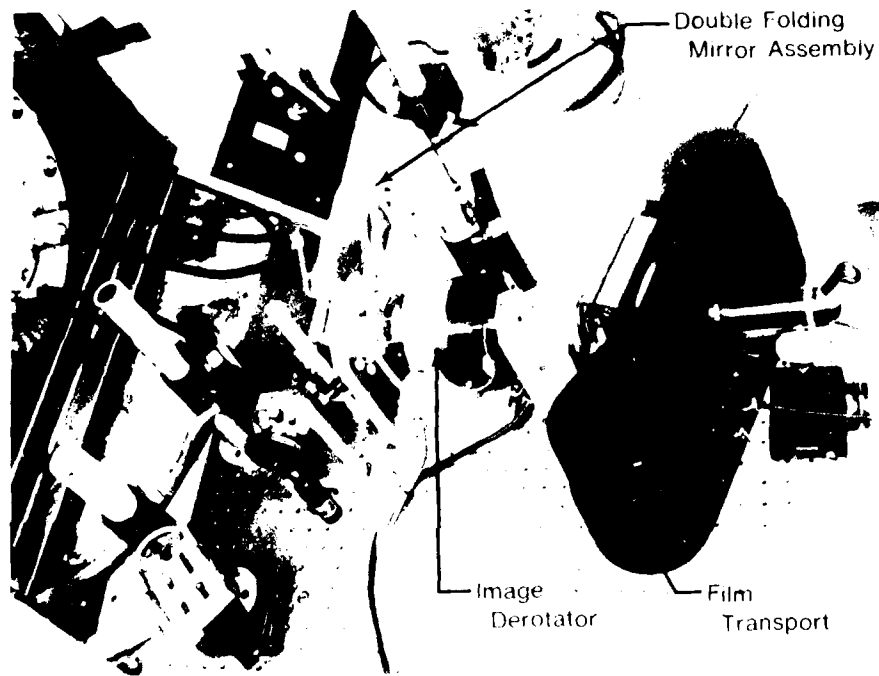
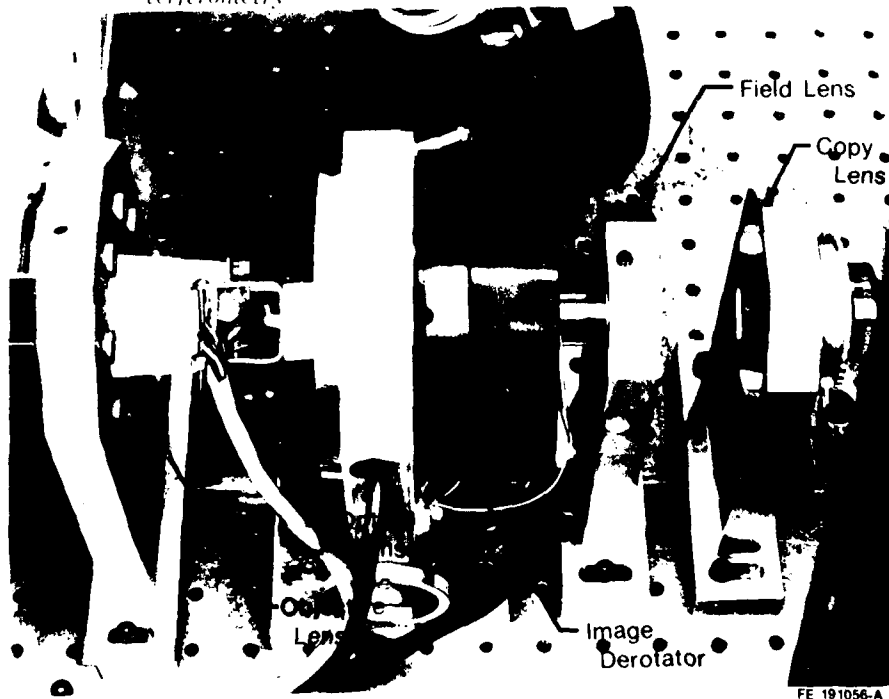


Figure 12. Experimental Setup for Image Derotated Holographic Interferometry in the Spin Test Facility



FE 191057-A

Figure 13. Optics Table Setup for Image Derotated Holographic Interferometry



FE 191056-A

Figure 14. Image Derotator With Objective, Field and Copy Lenses

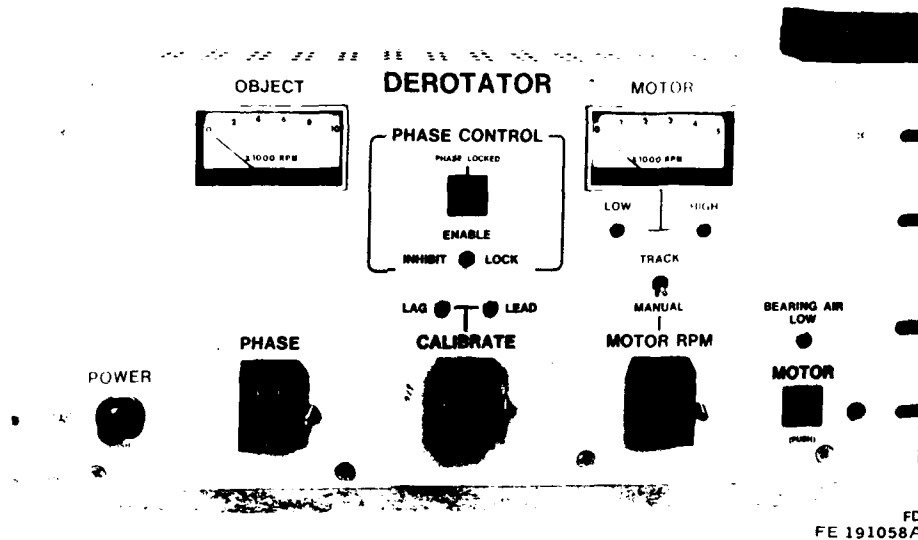
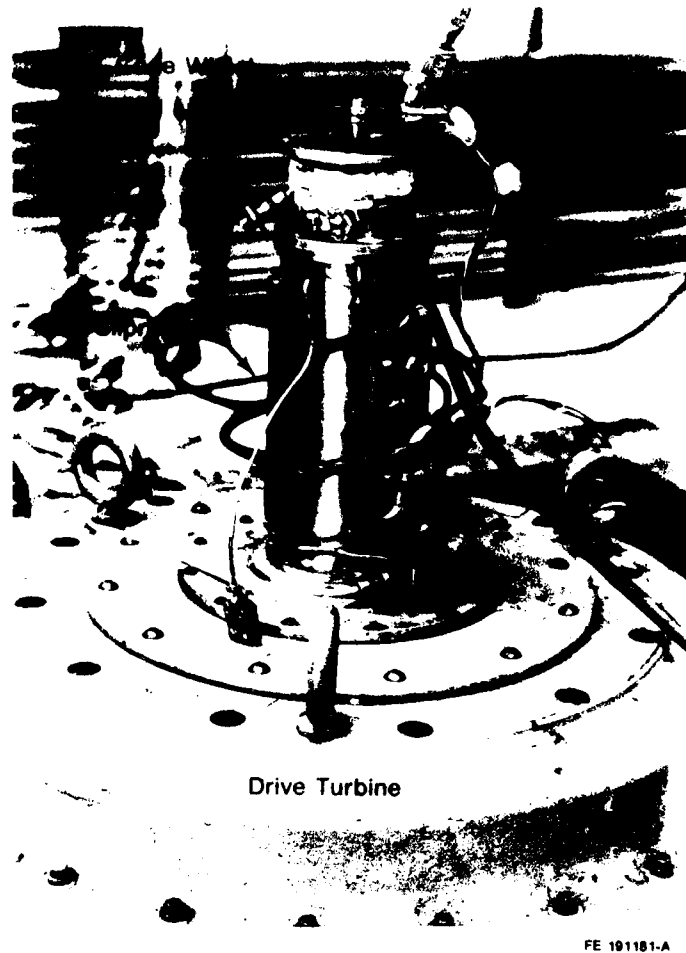


Figure 15. Image Derotator Control Unit

The output of the pulsed laser is monitored by a photo diode placed in the reference beam, and a Tektronix Model 7633 storage oscilloscope. When the laser is fired, a trigger signal from the laser power supply initiates the sweep of the oscilloscope trace, and the signal from the diode is recorded. This permits the monitoring of the relative output of the laser, if the laser emits a double pulse, and if so, a measure of the pulse separation.

### 3. STRAIN GAGE INSTRUMENTATION

The strain gage conditioning, monitoring, and analysis system is shown in Figure 17. The strain gages, mounted on the blades of the test structure, were routed through the drive shaft to a slipring on top of the air turbine. Unholtz-Dickie strain gage conditioning amplifiers were used to provide the gage excitation current and to amplify the strain gage signals. One gage was monitored on a real-time spectrum analyzer to establish when resonance occurred. The analyzer greatly facilitated the search for resonant modes of vibration of the bladed-disk by providing good definition between the magnet and slipring noise and the resonant response of the test structure. Strain gage data was recorded for 12 gages simultaneously on FM magnetic tape along with the pulsed laser trigger signal so strain data could be subsequently analyzed off-line for the same instant in time that the hologram was taken. The recorded data was analyzed on a Hewlett Packard Model 5451C FFT analyzer and frequency spectrum curves were established for each mode of vibration identified.

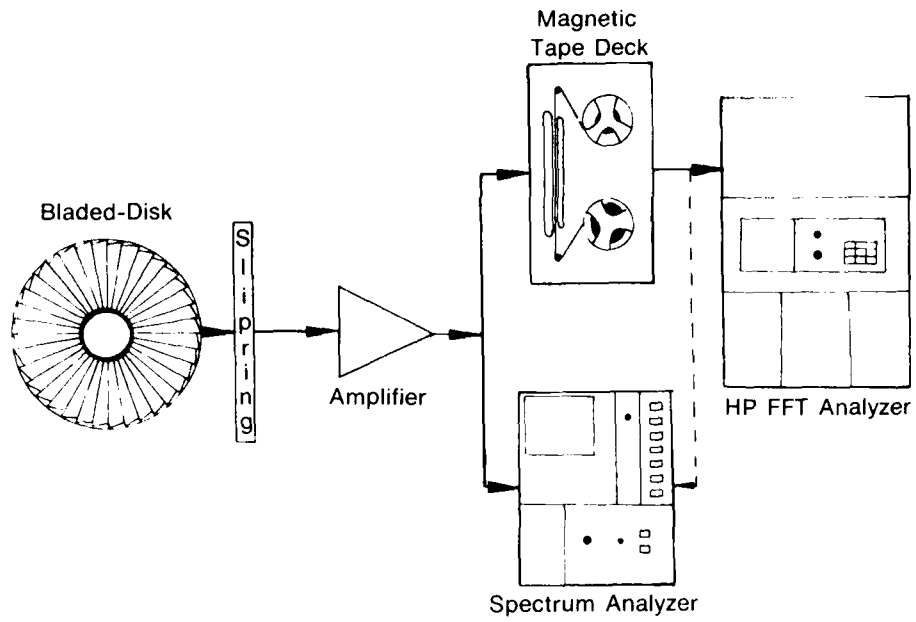


*Figure 16. Top of Spin Test Facility Showing Slipring, Code Wheel and Optical Sensor*

#### **4. ELECTROMAGNET EXCITATION SYSTEM**

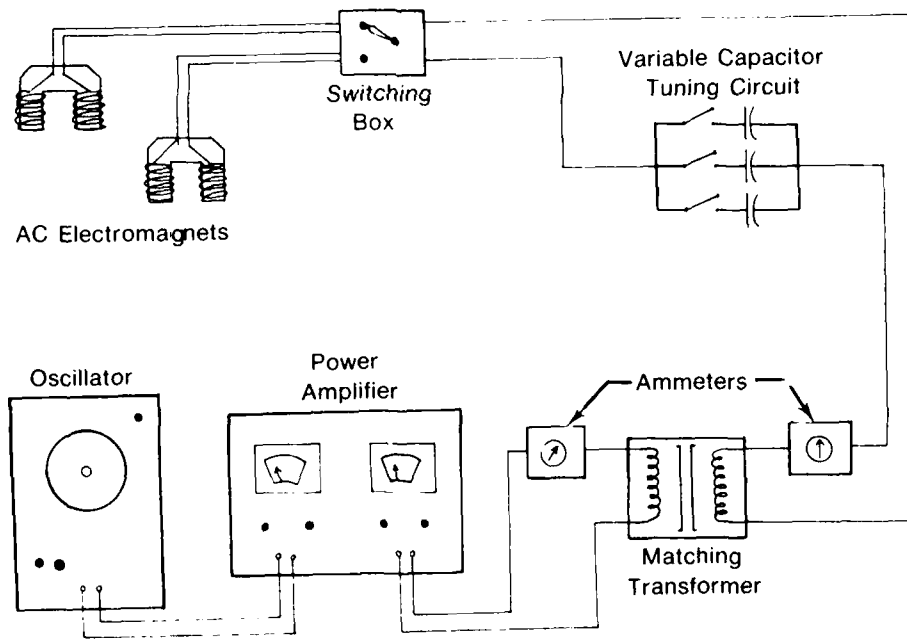
It was found early in the test program that excitation of the test structure with dc electromagnets was impractical. Therefore, only the system used to provide ac excitation throughout the remainder of the program will be discussed. The system, shown in Figure 18, consisted of an Altec Model 9440A 800-watt power amplifier, a transformer and variable capacitor bank, and two ammeters. The capacitor bank provided impedance matching between the amplifier and the magnets. The two ammeters were used to monitor the output of the amplifier and the input to the magnets so that the current limitations of each would not be exceeded.





FD 204182

Figure 17. Strain Gage Data Acquisition and Analysis Instrumentation



FD 204183

Figure 18. The ac Electromagnetic Excitation System

The ac electromagnets were fabricated at P&WA/GPD from 0.010-in.-thick steel sheets laminated together to provide electrical isolation between layers. Copper cooling lines were brazed to the outer surfaces of the magnets, and the magnets were then wound with 15-gauge copper magnet wire. The two magnets were wound with a different number of turns to provide optimum efficiency within separate frequency ranges. Although both magnets were mounted in the spit pit, as shown previously in Figure 2, only one was utilized at a time. An in-line switch outside of the spit pit allowed either one to be selected, depending on the frequency of the desired mode of vibration.

## SECTION IV

### HOLOGRAPHIC INTERFEROMETRY OF A ROTATING STRUCTURE

#### 1. TEST CONCEPT

With the development of advanced high-technology gas turbine engines, increasing emphasis has been placed on understanding the dynamic behavior of rotating structures. This behavior has been of interest ever since Campbell first theorized the response of a rotating structure in 1924 (Reference 3). However, it has only been within the past 10 yr that experimentation employing holographic techniques has permitted significant investigation of this phenomena.

Holographic interferometry methods developed to study the dynamic response of a rotating object can be categorized by three basic approaches: stroboscopic, rotating plate, and image derotated holographic interferometry (Reference 4). The first of these methods strobes the laser in synchronization with the rotating object so that it is illuminated at the same angular orientation after each revolution (References 5, 6, and 7). However, as the rotational speed of the object increases, the timing of the laser pulses becomes extremely critical, and the pulse width required to stop the rotary motion becomes exceptionally short. These difficulties limit the rotational speed of the object to less than 1500 rpm and, consequently, limit the usefulness of this method.

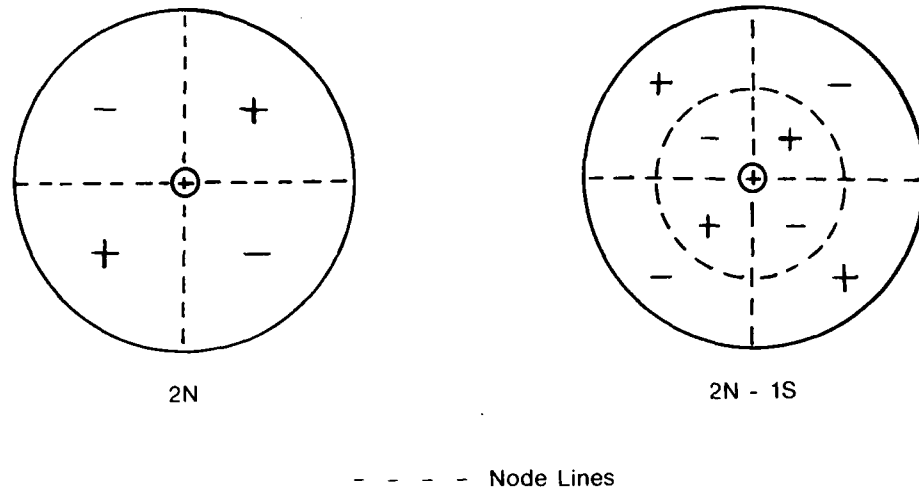
The rotating plate holographic interferometry method is accomplished by actually fixing the hologram to the rotating object along its axis of rotation (References 8 through 11). Since the holographic plate is rotating at the same speed as the object, all relative rotational motion is removed. Although this method has been used successfully to study a disk rotating up to 20,000 rpm, it has two basic disadvantages. First of all, it is not always possible to fix the hologram to the object, particularly if it is a gas turbine engine part, and secondly, the mechanical system used to hold the hologram must be extremely stable in order to prevent any vibration or rigid body motion of the hologram itself.

The image derotated holographic interferometry method that was first developed by P. Waddell (References 12 through 15) utilizes a rotating erector prism to optically stop the rotation of the object, thus producing a stationary image. Using a Q-switched double-pulsed ruby laser, double exposure holograms can be constructed of the dynamic response of the object. K. Stetson at the United Technologies Research Center developed the first practical optical image derotator (Reference 16). Stetson's derotator is a transmission configuration which uses a folded Abbe' prism. When the rotating object is viewed through the prism rotating at half the speed of the object, a stationary image is observed.

Stetson and MacBain (Reference 17) have conducted extensive analyses of small rotating disks using image derotated holographic interferometry techniques. Additionally, derotated holograms of a 1st-stage compressor bladed-disk of an engine running at speeds up to 7500 rpm in a test stand have been produced by Stetson. The program detailed in this report also applies derotated holographic interferometry techniques; however, it investigates the feasibility of establishing the dynamic behavior of turbine engine bladed-disks in a controlled laboratory spin test facility. Successful demonstration would provide a method of analyzing the dynamic behavior of any bladed-disk stage under controlled conditions of rotational speed and vibratory excitation.

## 2. RESONANT RESPONSE OF A ROTATING DISK

The resonant modes of vibration of a disk can be classified by the number of nodal diameters, node lines that extend diametrically across the disk; and nodal circles, node lines that extend circumferentially around the disk (depicted in Figure 19). The  $2N$  and  $2N-1S$  modes of a disk are shown where  $N$  refers to the number of nodal diameters, and  $S$  indicates the number of nodal circles.



FD 204184

Figure 19. Typical Mode Shapes of  $2N$  and  $2N-1S$  Modes of Vibration of a Circular Disk

First, consider the resonant response of a nonrotating disk excited by a sinusoidal force,  $P \cos \omega t$ , where  $P$  is the magnitude of the excitation force and  $\omega$  is the excitation frequency. The resultant displacement ( $W$ ), for the disk vibrating in a mode of vibration with  $n$  nodal diameters, can be described as a function of angular location ( $\theta$ ) and time ( $t$ ) (Reference 17):

$$W(\theta, t) = A \sin n\theta \cos p_n t \quad (1)$$

where

$A$  Resonant Amplitude  
 $p_n$  Resonant Frequency of  $n^{\text{th}}$  mode.

Equation 1 can be rewritten in the form

$$W(\theta, t) = \frac{A}{2} \sin(n\theta + p_n t) + \frac{A}{2} \sin(n\theta - p_n t) \quad (2)$$

If the disk is rotated at an angular velocity ( $\Omega$ ),  $\theta = \Omega t$  and, neglecting the stiffening effect of the centrifugal load on the disk, Equation 2 becomes

$$W(\theta, t) = \frac{A}{2} \sin [(p_n + n\Omega)t] + \frac{A}{2} \sin [(p_n - n\Omega)t] \quad (3)$$

Examination of Equation 3 reveals that resonance occurs when the excitation frequency ( $\omega$ ) is such that

$$\omega = p_n \pm n\Omega \quad (4)$$

Thus, a mode of vibration for a disk rotating at a specific rotational speed can be excited by two different excitation frequencies: one  $n\Omega$  greater and one  $n\Omega$  less than its nonrotating resonant frequency, as shown in Figure 20. It has been demonstrated (Reference 3) that excitation of the rotating disk at a frequency of  $p_n + n\Omega$  results in a mode shape that travels in the same direction as rotation of the disk, and excitation at  $p_n - n\Omega$  results in a mode shape traveling in a direction opposite to disk rotation. Of particular importance in gas turbine engines is the point at which the backward traveling wave has the same angular velocity in the opposite direction as the disk, or when

$$\Omega = \frac{p_n}{n}$$

This results in a standing wave that is stationary with respect to a point in space, and can be excited by a variance in the pressure field across a gas turbine engine bladed-disk.

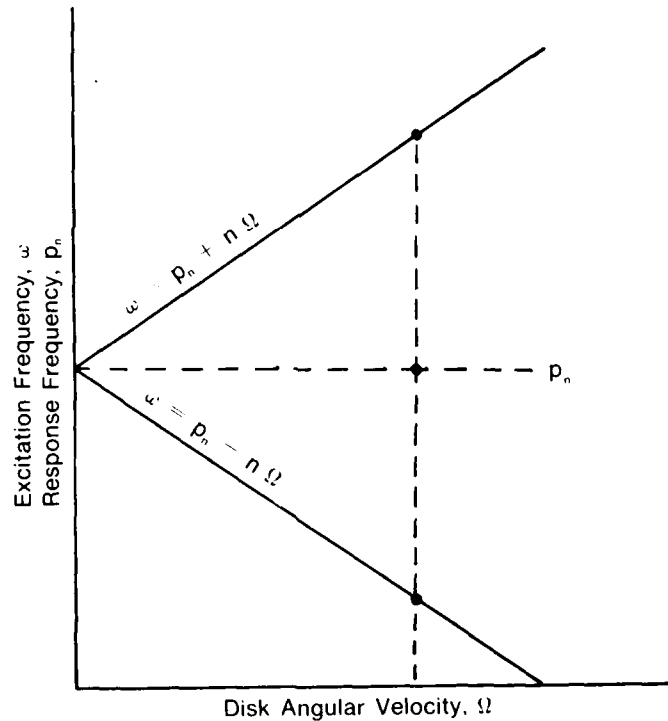


Figure 20. Excitation Frequencies for a Rotating Disk in the  $n^{\text{th}}$  Mode of Vibration With a Response Frequency of  $p_n$ .

### 3. EXCITATION METHOD

During the feasibility study and the first testing period of this program, excitation of the test structure was provided by two nonrotating dc electromagnets positioned 180 deg apart and, in this program, a magnetic ring with four raised steps equally spaced around the ring which was bolted to the disk. As the bladed-disk rotated with the magnetic ring in close proximity to the magnets, a four-pulse-per-revolution input excitation resulted. It was demonstrated during the feasibility study (Reference 2) that for a pulsed excitation, the forcing frequency was related to the angular velocity of the bladed-disk by  $\omega = mk\Omega$ ; where  $m$  is the number of pulses per revolution of the disk, and  $k$  is a positive integer ( $4k\Omega$  for this particular case). Rearranging and substituting into Equation 4, it can be seen that resonance of the  $n$ th diameter mode will occur when

$$p_n = 4k\Omega + n\Omega$$

or

$$p_n = (4k + n)\Omega \quad (5)$$

As can be seen from Equation 5 and Figure 21, taken from the feasibility results, the excitation of each mode of vibration for the F100 2nd-stage turbine disk occurs at only a few discrete rotational speeds.

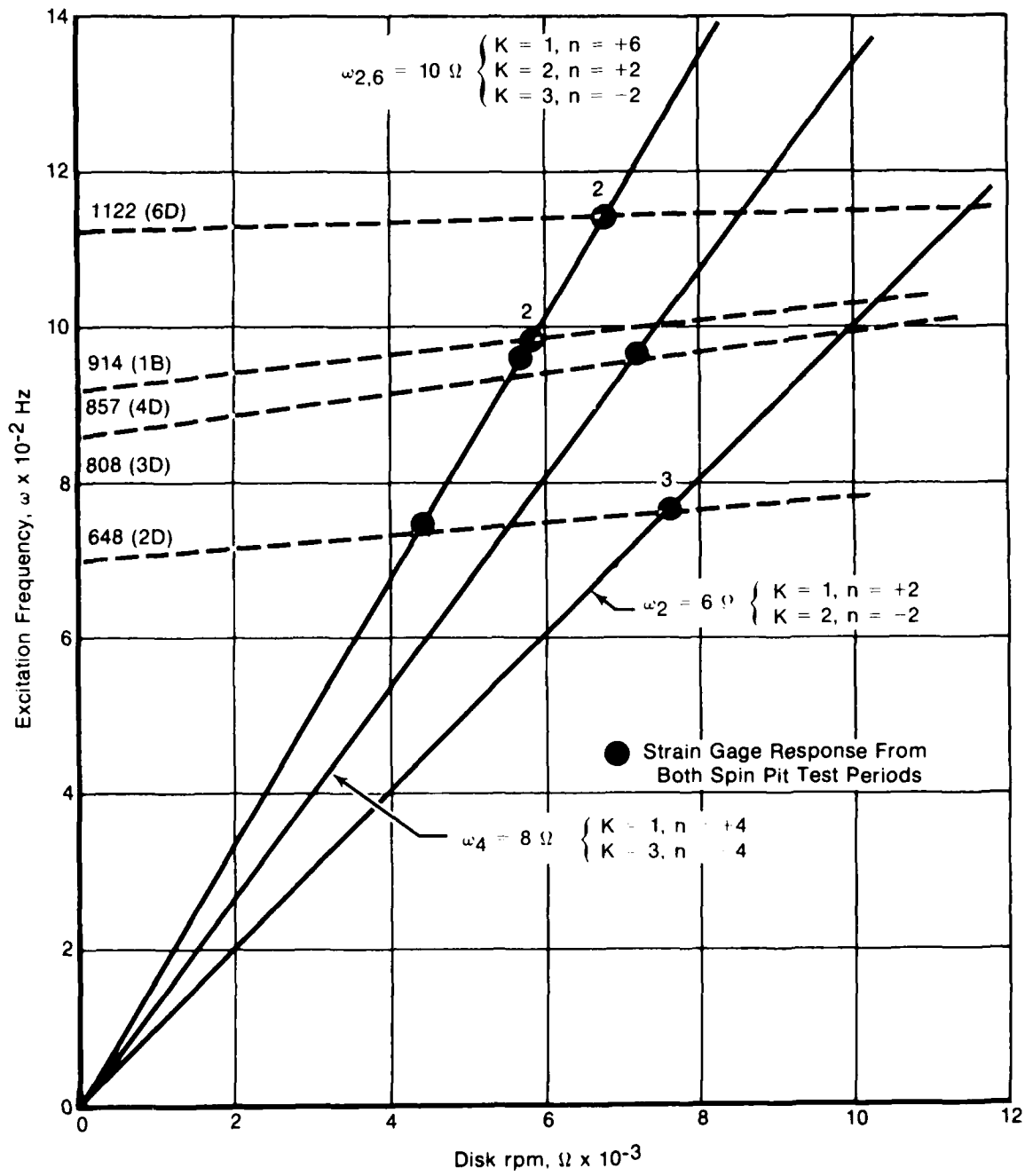
The rotational speed dependence of dc excitation proved to be an extreme disadvantage early in the program for two reasons. First, the bladed disk was a lightly damped structure which required that a precise rotational speed be maintained to excite a resonance near its maximum response. Accomplishing this precision in controlling the speed was difficult since any fluctuation in air pressure at the drive turbine resulted in a corresponding fluctuation of the rotational speed of the bladed-disk. Secondly, any rotating structure, particularly one that is supported at only one end as is the case in the spin pit, tends to spin in a more stable fashion at certain speeds and less stable at others. If a desired mode of vibration is excited at a speed where the test structure is spinning unstably, hologram construction of the mode becomes extremely difficult.

For the above reasons, the decision was made to switch to ac electromagnets, thus providing sinusoidal excitation of the bladed-disk. This had the immediate benefit of making it possible to select a rotational speed at which the bladed-disk would spin with stability, and then tune the excitation frequency to excite either the forward or backward traveling waves of any mode of vibration. If the speed of the bladed-disk did change, the excitation frequency could easily be retuned to compensate for the speed change.

### 4. EXPERIMENTAL TECHNIQUE

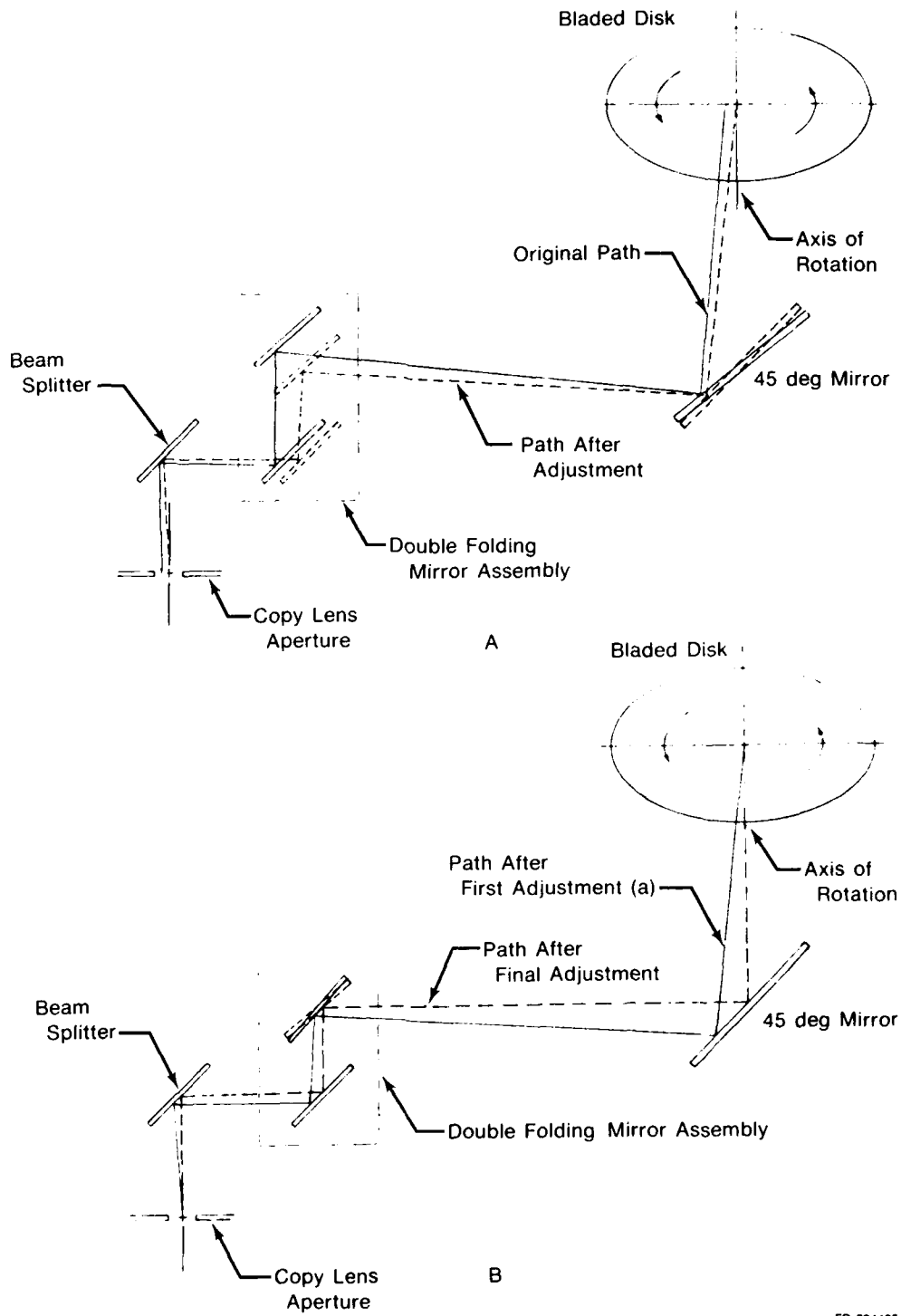
The experimental technique utilized during this program involved the development of methods for the optical alignment of the image derotator system with the test structure in the spin pit, excitation of the rotating bladed-disk, and construction of image derotated double exposure holograms of the resonance response of the bladed-disk.

The procedure for alignment of the axis of rotation of the derotator and the rotating test structure was basically the same as that developed by Stetson, but with some modification dictated by differences in the experimental apparatus. During alignment, a 50 mw helium-neon laser was utilized to illuminate the test structure, and a low-power microscope with a cross hair reticle was placed just behind the film plane to visualize the laser speckle pattern. The alignment involved just two basic steps, as illustrated in Figure 22. However, each of these basic steps had to be repeated several times for three different test conditions: at low rotational speed of the bladed-disk, at high rotational speed, and with the electromagnet excitation on.



FD 147969

Figure 21. Experimental Results With de Magnetic Excitation Taken from the Feasibility Study of the F100 2nd-Stage Turbine Disk



FD 204186

Figure 22 Procedure for Optical Alignment of Axes of Rotation for the Bladed-Disk and Image Derotator: (a) Adjustment of 45-deg Mirror and Translation of Double-Folding Mirrors To Center the Two Axes of Rotation, and (b) Tilting of the Upper Mirror in the Double-Folding Mirror Assembly To Make the Two Axes Coincidental



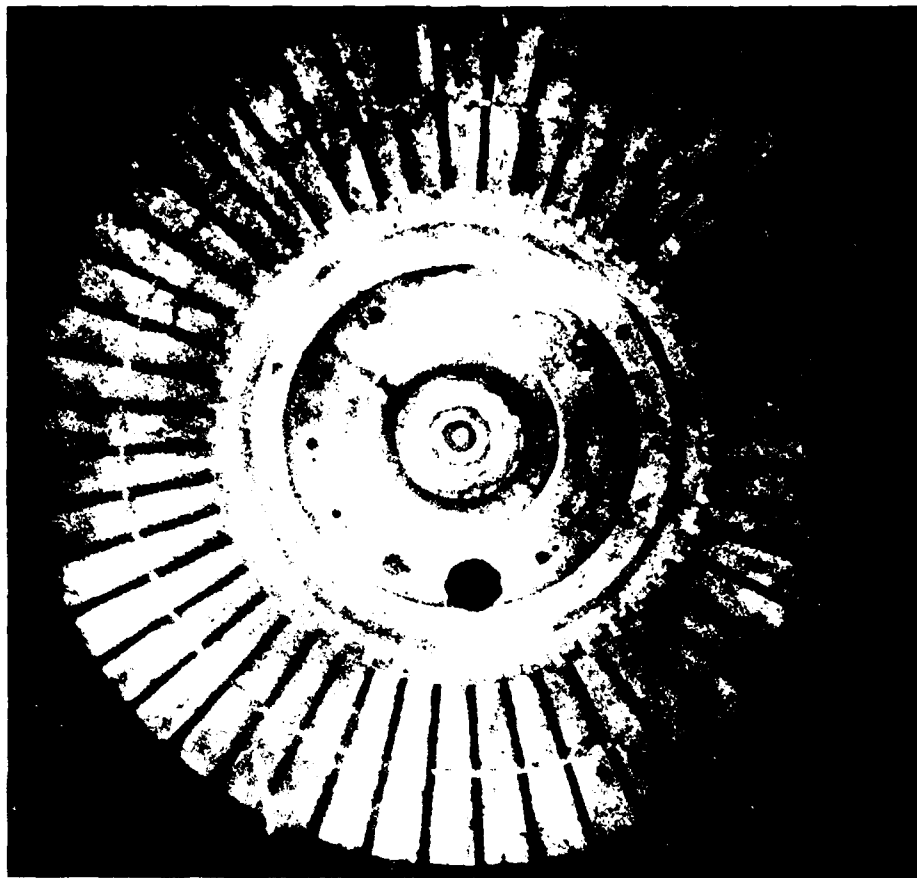
The first step (Figure 22a) was to align the axis of rotation of the derotator in the plane of the bladed-disk. To accomplish this, the microscope was focused on the partially stopped down copy lens aperture, and the laser speckle pattern in this plane visualized. As the derotator was rotated slowly by hand, the speckle pattern was seen to rotate about a center, and the microscope could be translated to locate the center of speckle on the cross hair. With the derotator stationary, the bladed-disk was then rotated slowly (less than 1000 rpm), and the resultant center of speckle centered on the microscope cross hair by adjustment of the large 45-deg mirror inside the spin pit and the vertical and horizontal translators of the double-folding mirror (Figure 13). The hydraulically adjustable mount for the 45-deg mirror greatly facilitated this procedure, since a rough alignment could be achieved with the 45-deg mirror, and the double-folding mirrors were reserved for fine alignment.

The second step (Figure 22b) was to rotate the axis of the derotator to make it coincident with the axis of rotation of the test structure. This was accomplished by derotating the bladed-disk and focusing the microscope on the object. The speckles observed on the bladed-disk appeared in the form of circles. The upper mirror of the double folding mirror assembly could then be rotated to reduce the speckle circles to points. Since these two alignment steps affect each other, they had to be repeated several times until the alignment converged.

Since the drive shaft rotating the test structure is supported only at the top of the drive turbine, the axis of rotation of the structure is allowed to shift as the rotational speed is increased. Therefore, after the low-speed alignment was completed, it was necessary to repeat the procedure at the speed at which holograms were to be constructed. Since the rotation of the speckle pattern at the copy lens aperture was not discernible at rotational speeds of the test structure above 1000 rpm, a method of alignment at higher speeds had to be devised. The high-speed alignment was accomplished by strobing the helium-neon laser beam at a frequency just slightly less than that of the rotating bladed-disk. The center of speckle could then be observed and aligned. Excellent results were achieved using this technique for rotational speeds up to 9000 rpm, as shown in Figure 23. However, only a slight instability in the spin of the test structure could be tolerated, or an inexact alignment resulted which produced a set of parallel bias fringes on the holograms (depicted in Figure 24). Therefore, a good balance of the test structure before mounting in the spin pit was imperative to minimize the spin instability.

As the electromagnetic excitation was applied to the test structure, the resultant pull on the bladed-disk shifted its axis of rotation. The final step in the alignment procedure was, therefore, the adjustment in alignment to compensate for this shift. This final alignment was performed at the same rotational speed as the high-speed alignment and with the current input to the electromagnet the same as would be used during hologram construction.

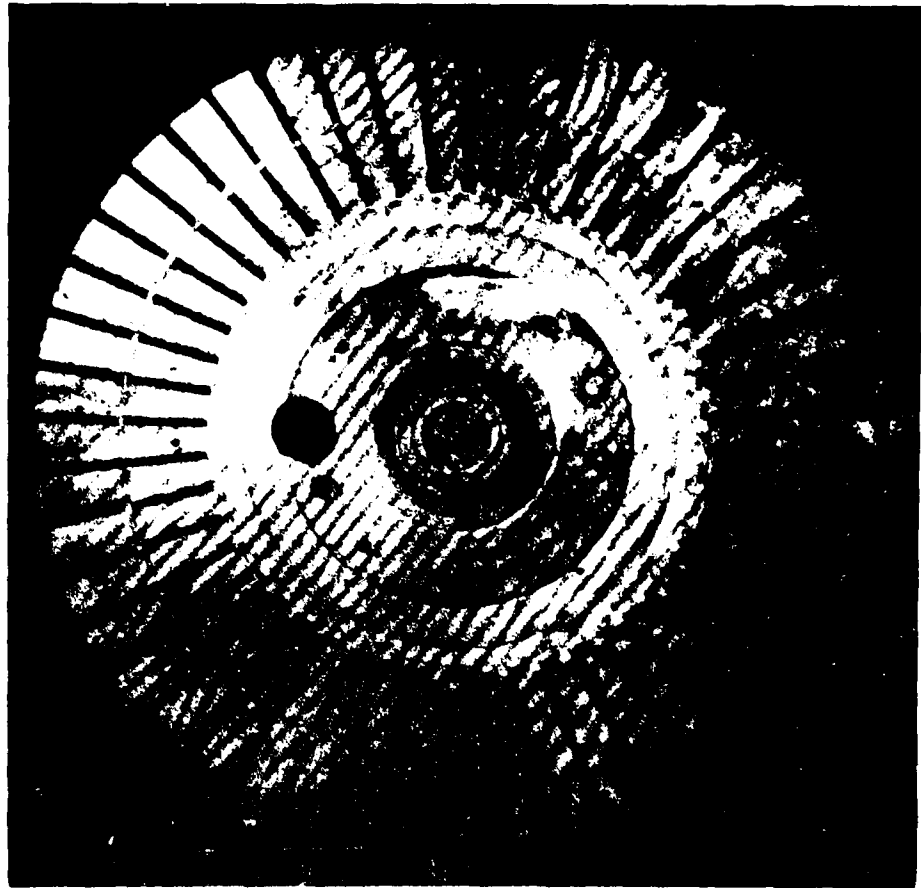
Excitation of the rotational test structure was accomplished using the ac electromagnetic system described in Section III. As the frequency of excitation was varied, the impedance match between the power amplifier and the magnet changed, thus lowering the effective current that could be applied to the magnet. The magnet circuit had to be retuned using the in-line variable capacitance circuit to compensate for the change in impedance. A strain gage monitored on-line with a spectrum analyzer was used to establish when resonance of the bladed-disk occurred. The spectrum analyzer greatly facilitated this effort, since the resonant response of the bladed-disk could be easily discerned from an unfiltered strain gage signal that also contained magnet and slipring-induced noise. A reduction in the rapid induction heating of the test structure due to the interaction of the electromagnets and the magnetic ring was evident with the switch from dc to ac electromagnetic excitation. However, this continued to be a problem, and a continuous monitoring of the thermocouples attached to the disk had to be maintained to keep the temperature of the disk below 300°F to avoid damage to the strain gages.



*Figure 23. Image Derotated Double Exposure Hologram of J52 2nd-Stage Compressor Bladed-Disk Rotating at 9000 rpm With No Vibratory Excitation (Pulse Separation Was 40 $\mu$  sec)*

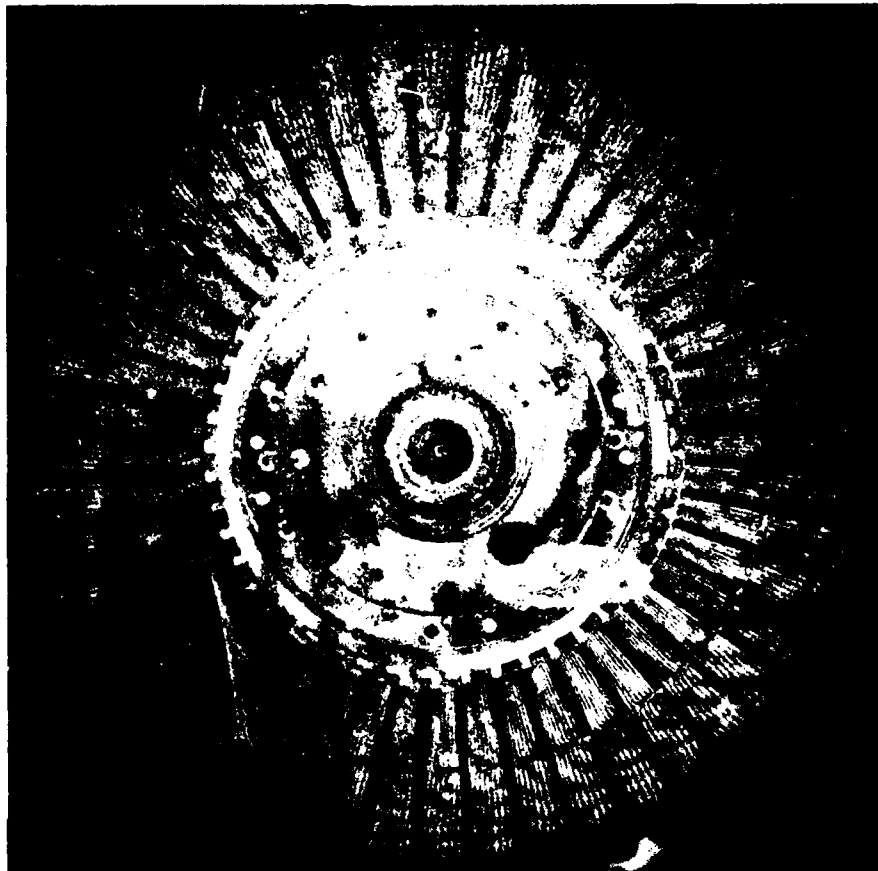
At least two unwanted excitation sources were detected during this program although their effect was minimal. The excitation at the rotational speed of the test structure at 1E, due to the rotor imbalance, was low in amplitude and for the most part below the frequency range of interest. The other, that was thought to be a resonance in the drive system, occurred at only one discrete rotational speed and was easily avoided.

Image derotated holograms were constructed for the resonant responses of the rotating test structure with the double-pulsed ruby laser. A pulse separation of 40 $\mu$  sec was used for most of the testing program to minimize the misalignment bias fringes. However, once the alignment procedure was fully developed, a longer pulse separation could have been used if a stable spin of the test structure had been achieved. Sufficient excitation was available, however, that even with the short pulse separation, the fringe density on the holograms was adequate to identify the modes of vibration of the bladed-disk.



*Figure 24. Image Derotated Double Exposure Hologram Showing Misalignment Bias Fringe Pattern (Pulse Separation Was  $40\mu$  sec)*

Once the alignment procedure was developed, most of the problems encountered in the construction of the image derotated holograms were due to the pulsed laser. The most recurrent of the laser problems was the multimoding of the laser that imparted contour fringes on the holograms, as shown in Figure 25. Attempts to rectify this problem met with limited success.

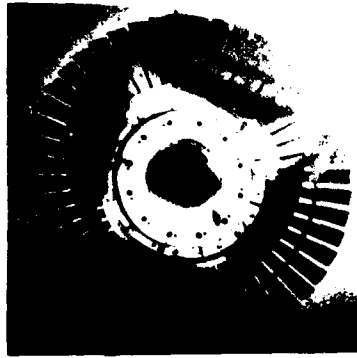


*Figure 25. Image Derotated Double Exposure Hologram of J52 2nd-Stage Compressor Bladed-Disk Showing Contour Fringes Resulting from Multimoding of Double Pulsed Ruby Laser*

## **5. DATA ANALYSIS**

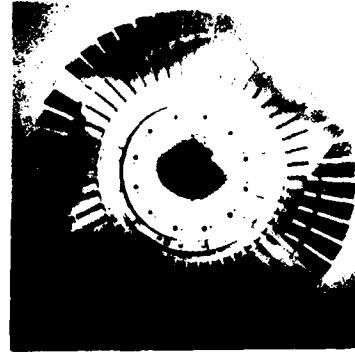
Before the rotational analysis of the J52 2nd-stage compressor bladed-disk was initiated, a nonrotating holographic analysis was conducted. The resultant reconstructed time average holograms are shown in Figure 26.

Three modes of vibration of the bladed-disk that were identified during the nonrotating holographic analysis (the 2N, 2N-1S, and 3N-1S modes), and one that was not (the 1N-1S mode) were excited with the bladed-disk rotating at various rotational speeds, as shown in Table I and Figure 27. The sinusoidal excitation provided by the ac electromagnets made it possible to demonstrate the capability of exciting either the forward or backward traveling waves of a mode, as discussed in Section IV. The stiffening effect of the centrifugal load on the test structure can also be seen in Figure 27, as evidenced by the nonlinear increase in both the response and excitation frequencies.



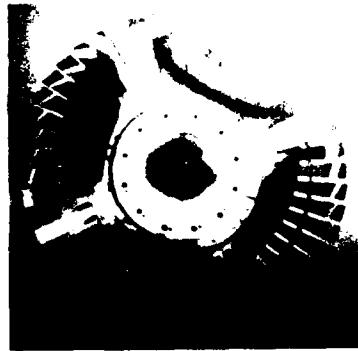
2N

290 Hz



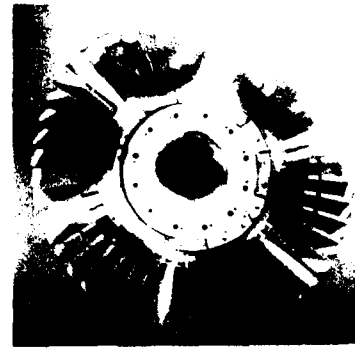
3N

348 Hz



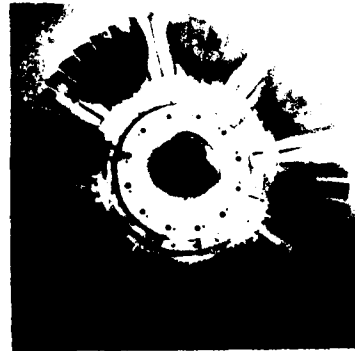
2N-1S

460 Hz



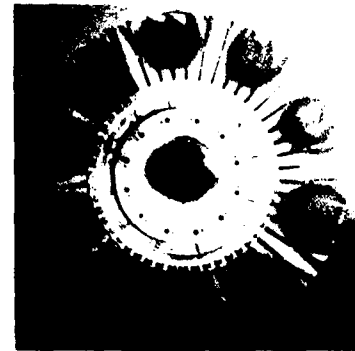
3N-1S

596 Hz



4N-1S

811 Hz



5N-1S

970 Hz

FD 204187

*Figure 26. Reconstructed Time Average Holograms of Nonrotating J52 2nd-Stage Compressor Bladed-Disk*

TABLE 1. RESONANT RESPONSES OF THE J52 2ND-STAGE COMPRESSOR BLADED-DISK ROTATING IN THE SPIN TEST FACILITY

<i>Bladed-Disk Rotational Speed (rpm)</i>	<i>Excitation Frequency (Hz)</i>	<i>Response Frequency (Hz)</i>	<i>Mode of Vibration</i>
5000	365	528	2N-1S
	380	628	3N-1S
	468	395	1N-1S
	500	342	2N
7000	310	657	3N-1S
	334	565	2N-1S
	538	420	1N-1S
	592	365	2N
	794	562	2N-1S
7500	296	674	3N-1S
	300	670	3N-1S
	544	422	1N-1S
	550	425	1N-1S
	620	370	2N
	820	572	2N-1S
8000	852	585	2N-1S
8500	270	684	3N-1S

Image derotated double exposure holograms were constructed for three of the four resonant modes of vibration identified with the bladed-disk rotating at speeds between 7000 and 7500 rpm. Reconstructed photographs of a few of the holograms are evidenced in Figures 28 through 33. Typical spectral response curves of the unfiltered signals from several of the highest responding strain gages are presented in Figures 34 through 38.

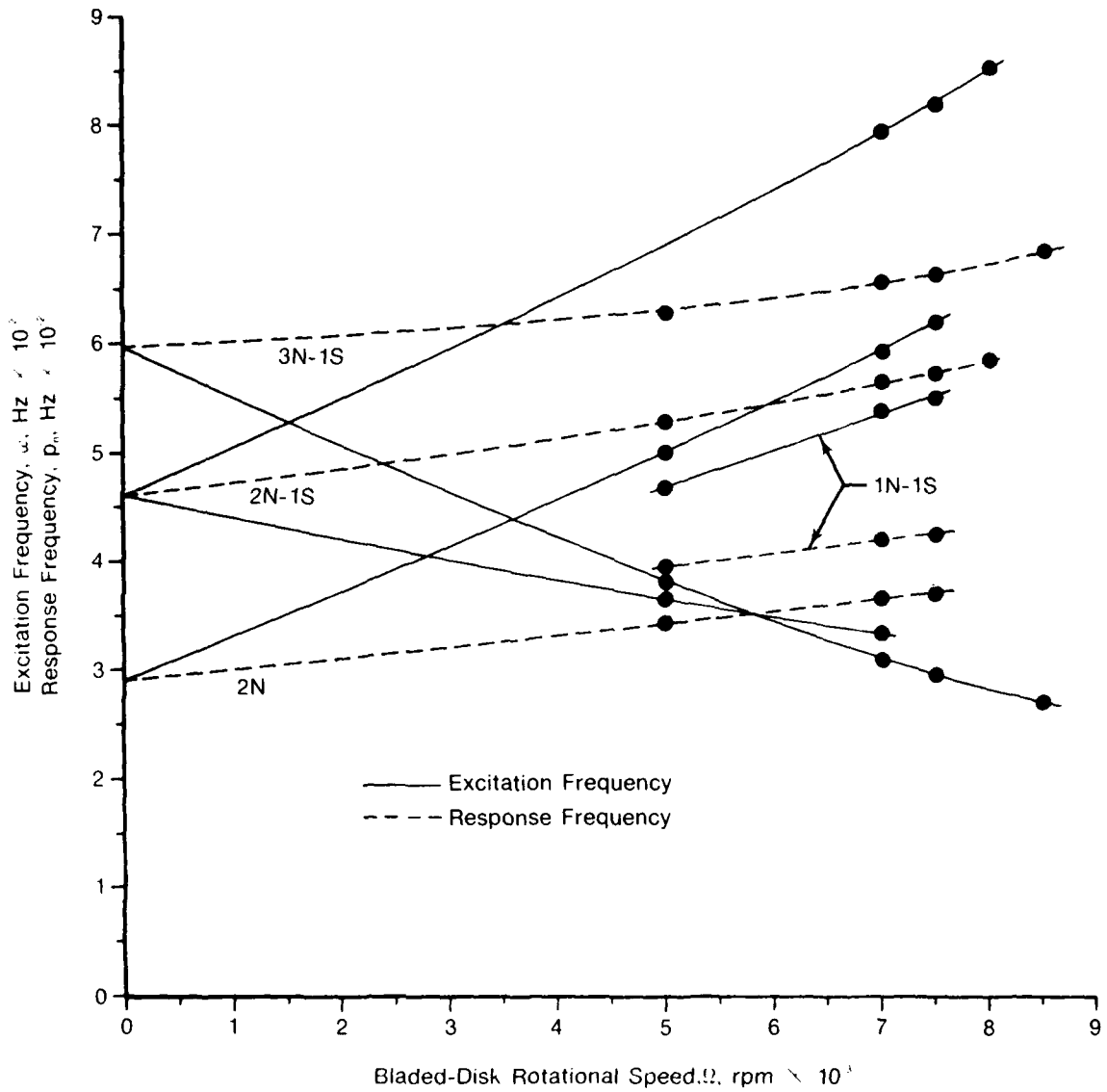


Figure 27. Excitation and Response Frequencies as a Function of Bladed-Disk Rotation Speed for the 2N, 1N-1S, 2N-1S and 3N-1S Modes of Vibration

FD 204188



*Figure 28. Image Derotated Double Exposure Hologram of the 3N-1S Mode of Vibration of the J52 2nd-Stage Compressor Bladed-Disk Rotating at 7500 rpm (the Excitation Frequency was 300 Hz and the Response Frequency was 670 Hz)*



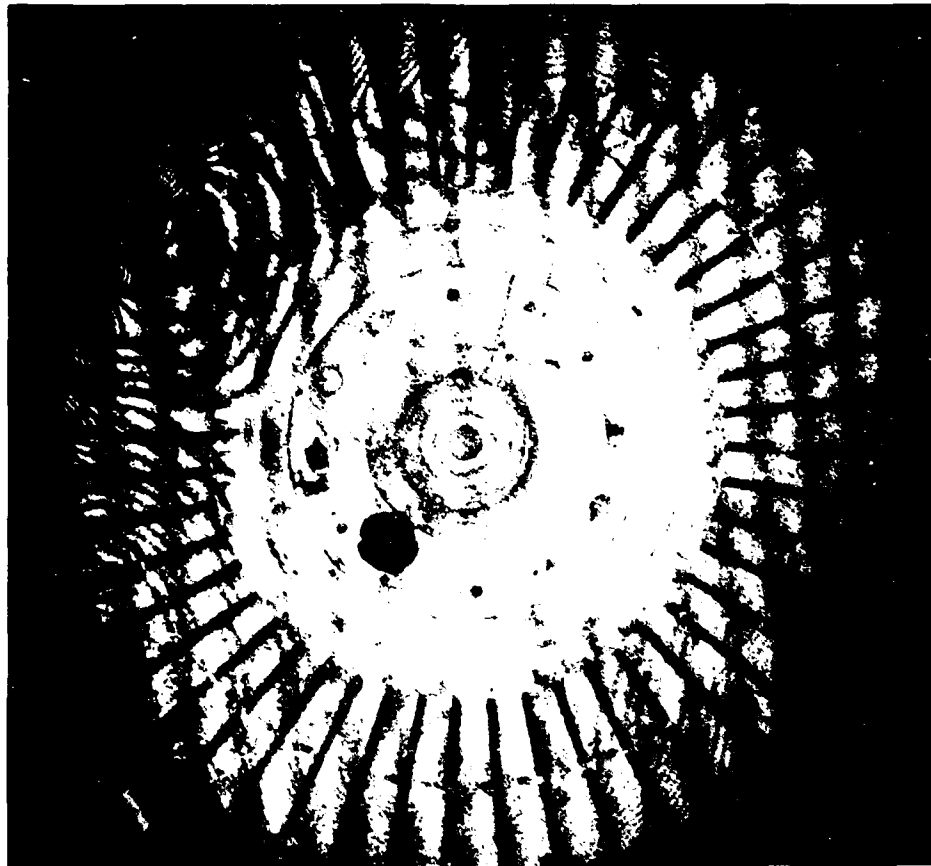


*Figure 29. Image Derotated Double Exposure Hologram of the 3N-1S Mode of Vibration of the J52 2nd-Stage Compressor Bladed-Disk Rotating at 7500 rpm (the Excitation Frequency was 296 Hz and the Response Frequency was 674 Hz)*

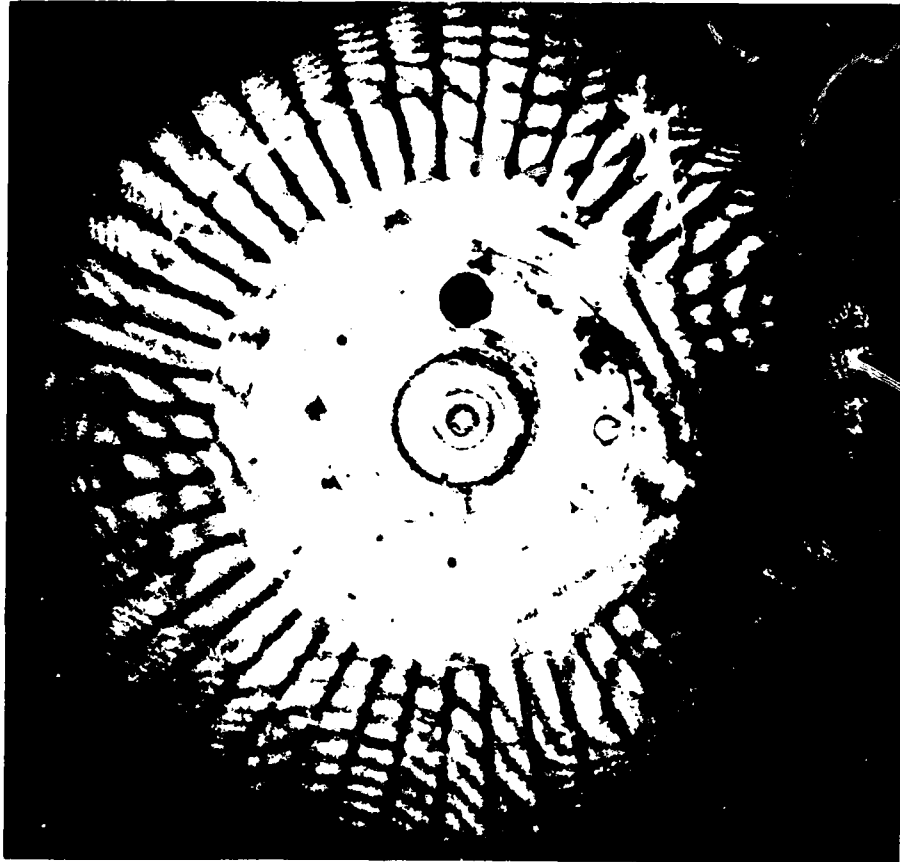


*Figure 30. Image Derotated Double Exposure Hologram of the 3N-1S Mode of Vibration of the J52 2nd-Stage Compressor Bladed-Disk Rotating at 7000 rpm (the Excitation Frequency was 310 Hz and the Response Frequency was 657 Hz)*

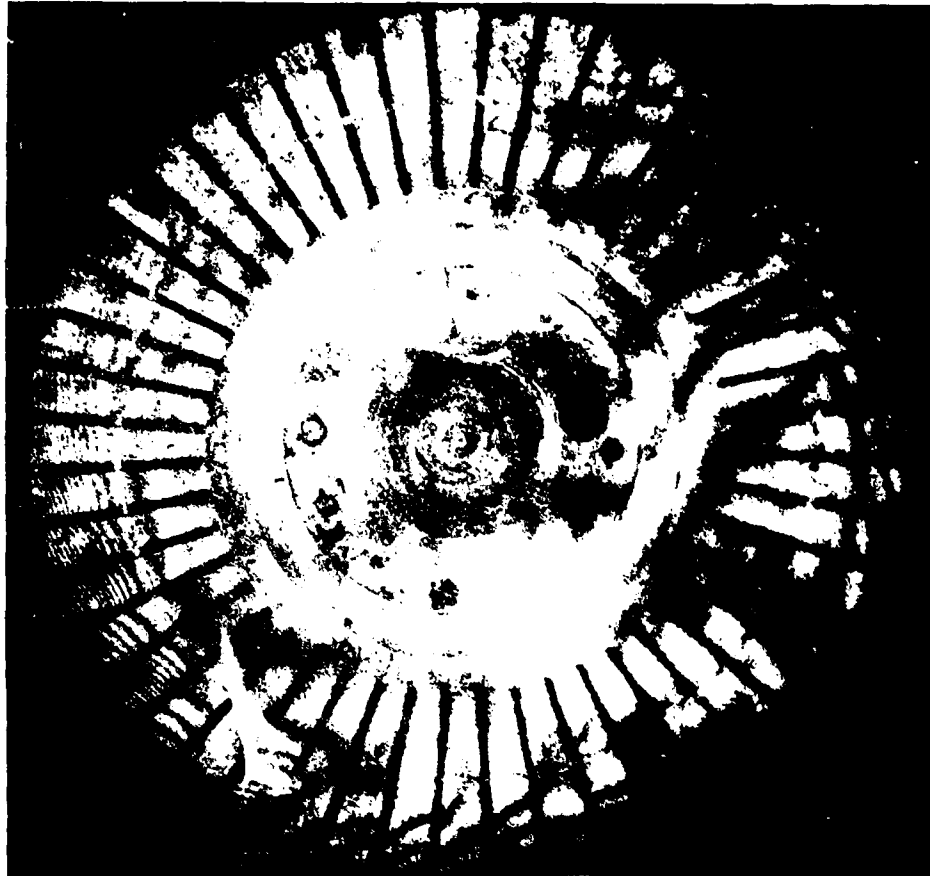


*Figure 31. Image Derotated Double Exposure Hologram of the 1N-1S Mode of Vibration of the J52 2nd-Stage Compressor Bladed-Disk Rotating at 7500 rpm (the Excitation Frequency was 550 Hz and the Response Frequency was 425 Hz)*

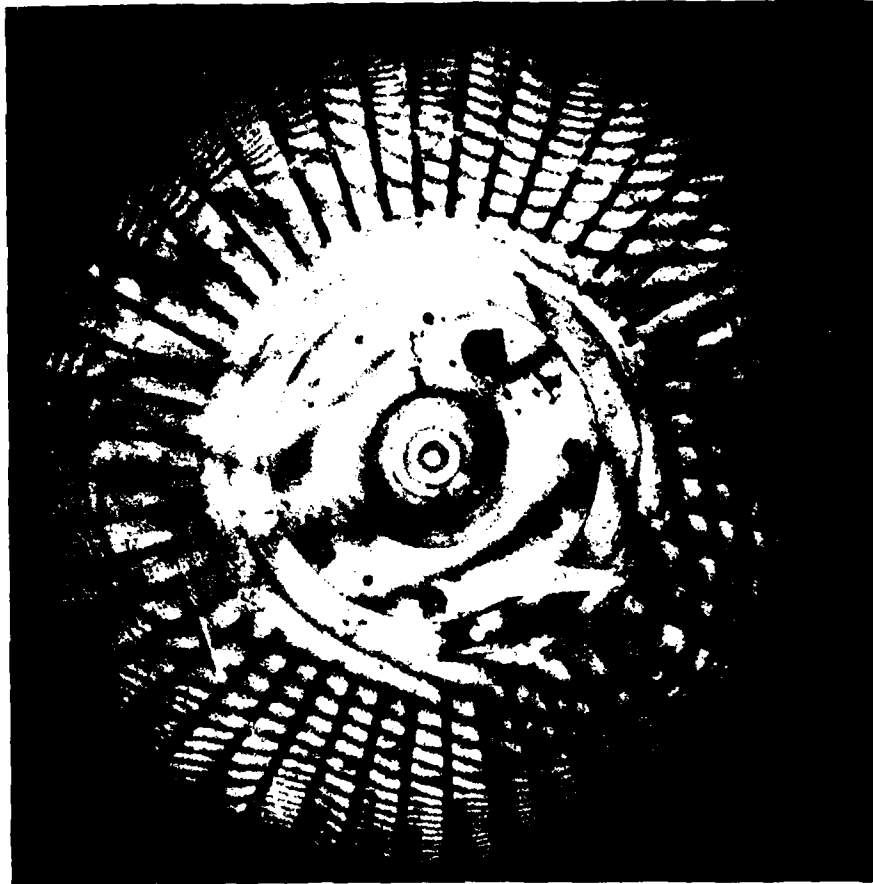
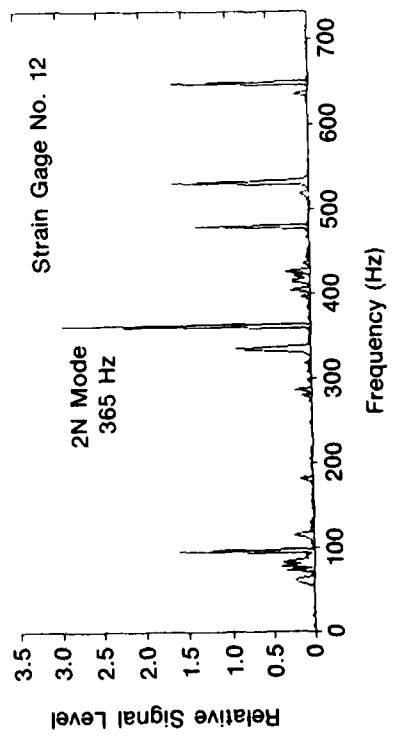
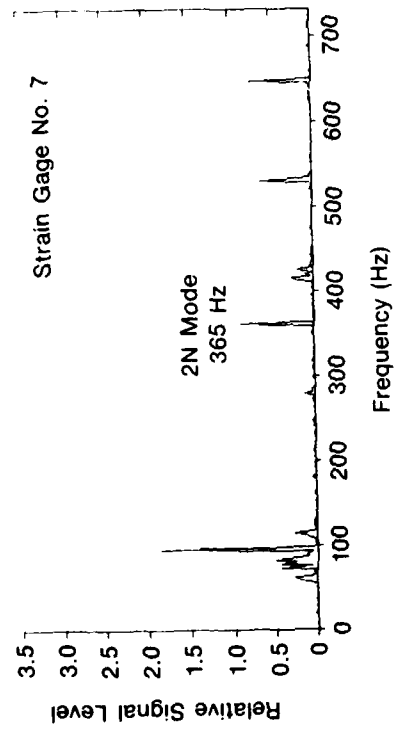
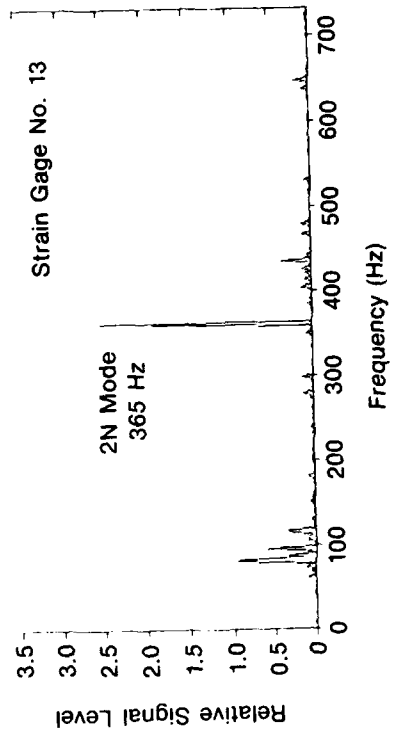
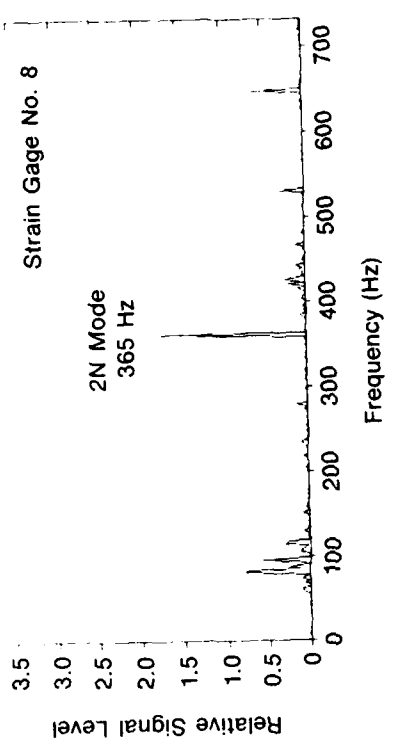


*Figure 32. Image Derotated Double Exposure Hologram of the 1N-1S Mode of Vibration of the J52 2nd-Stage Compressor Bladed-Disk Rotating at 7500 rpm (the Excitation Frequency was 544 Hz and the Response Frequency was 422 Hz)*



*Figure 33. Image Derotated Double Exposure Hologram of the 2N Mode of Vibration of the J52 2nd-Stage Compressor Bladed-Disk Rotating at 7500 rpm (the Excitation Frequency was 620 Hz and the Response Frequency was 370 Hz)*



FD 204189

Figure 34. Spectral Response Curves for the Indicated Strain Gages Mounted on a J52 2nd-Stage Compressor Bladed-Disk Rotating at 7000 rpm and Excited in the 2N Mode of Vibration With an Excitation Frequency of 592 Hz

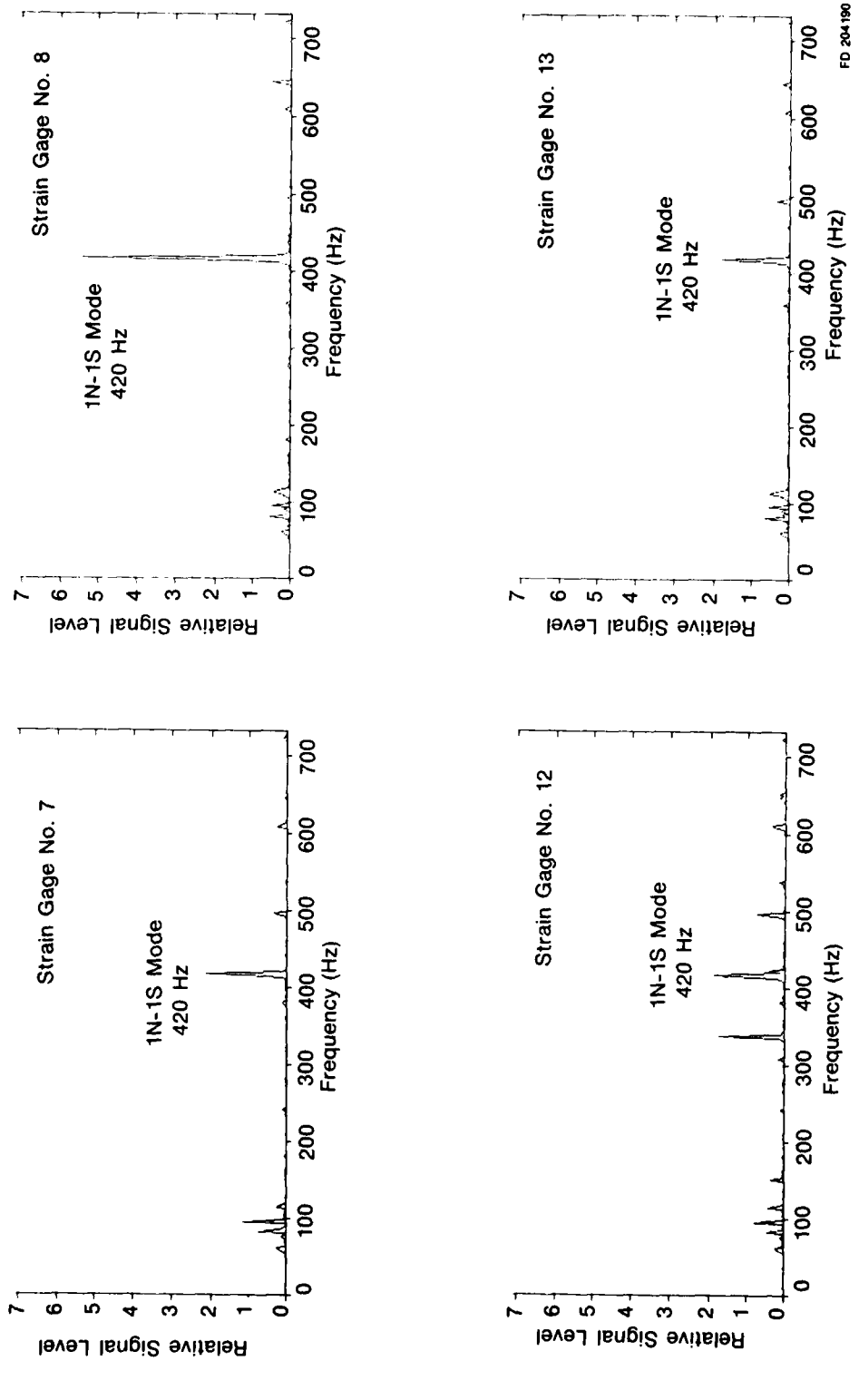
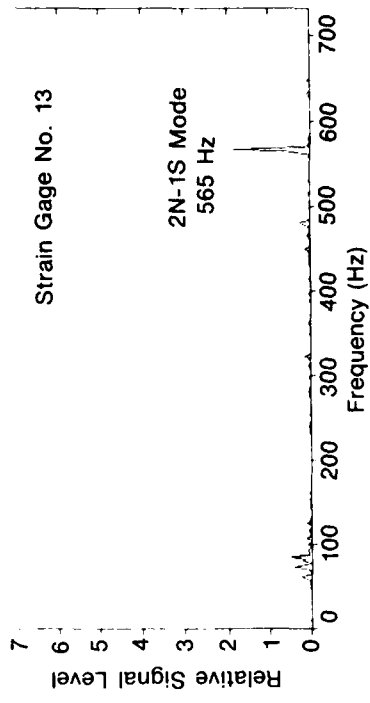
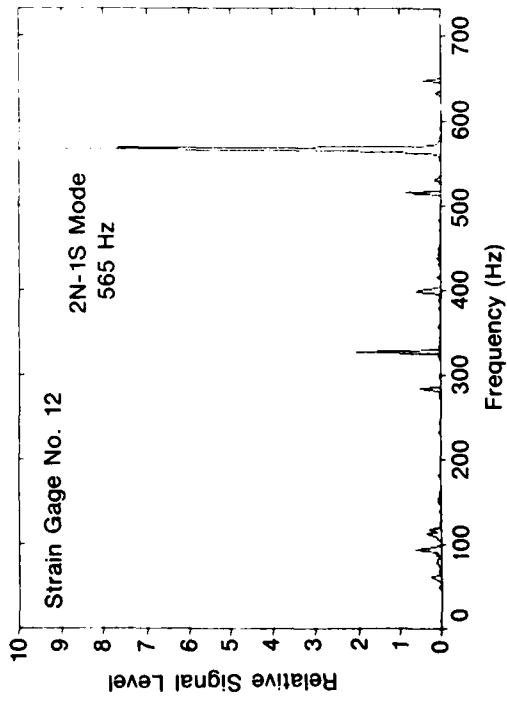
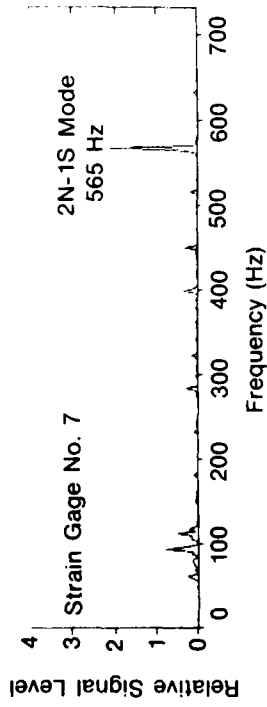
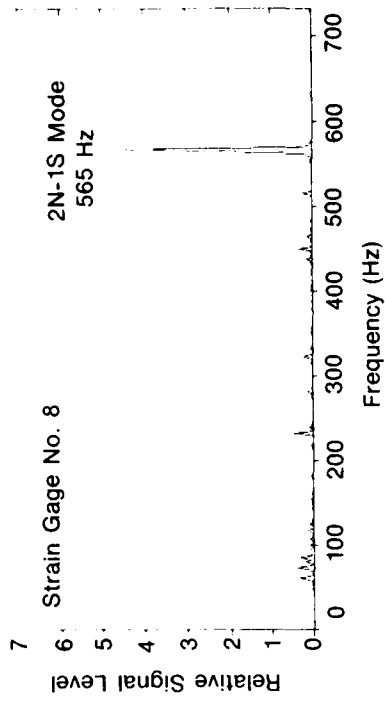


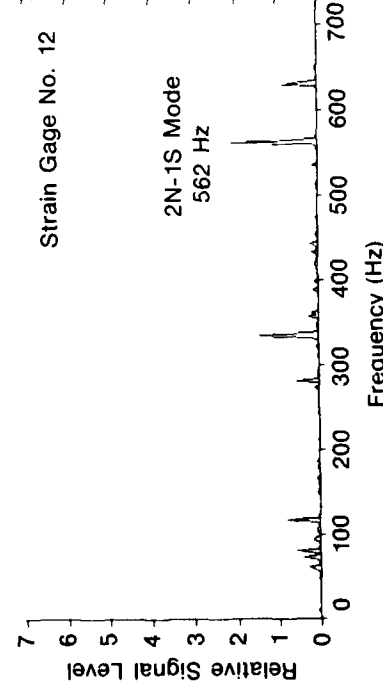
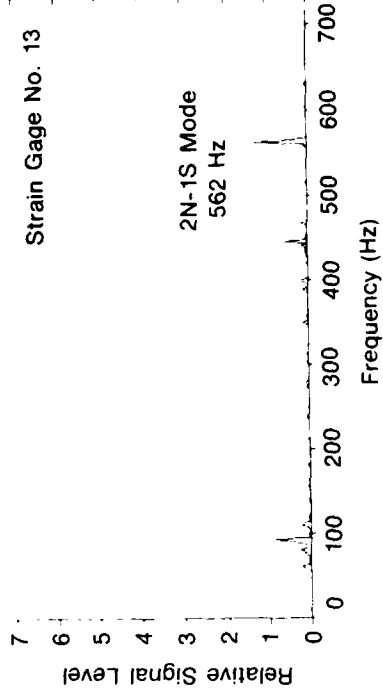
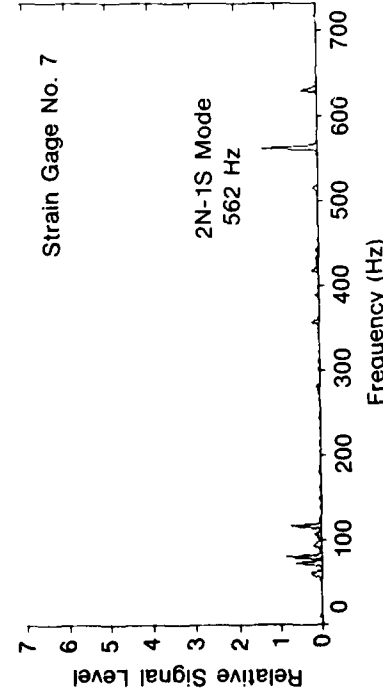
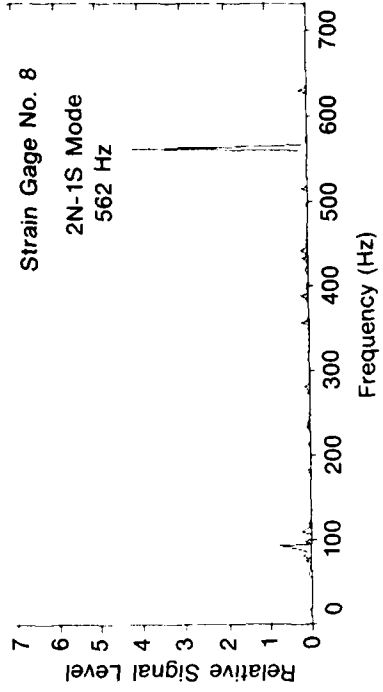
Figure 35. Spectral Response Curves for the Indicated Strain Gages Mounted on a J52 2nd-Stage Compressor Bladed-Disk Rotating at 7000 rpm and Excited in the 1N-1S Mode of Vibration With an Excitation Frequency of 538 Hz



FD 204191

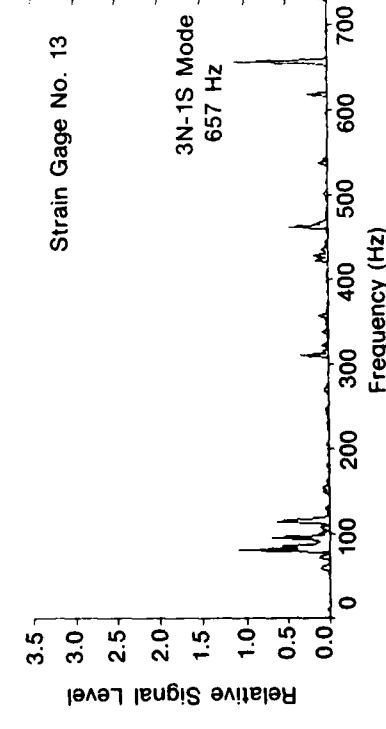
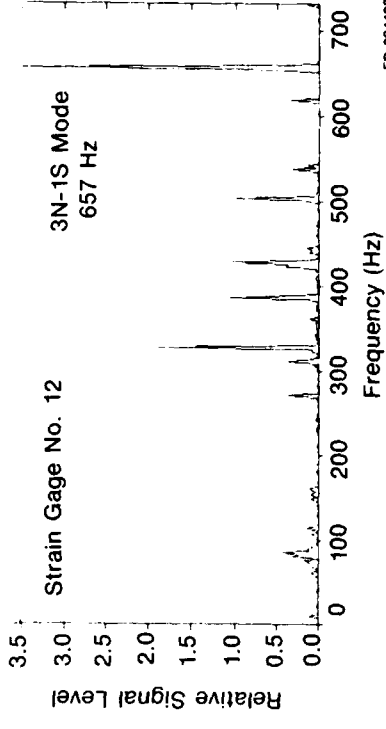
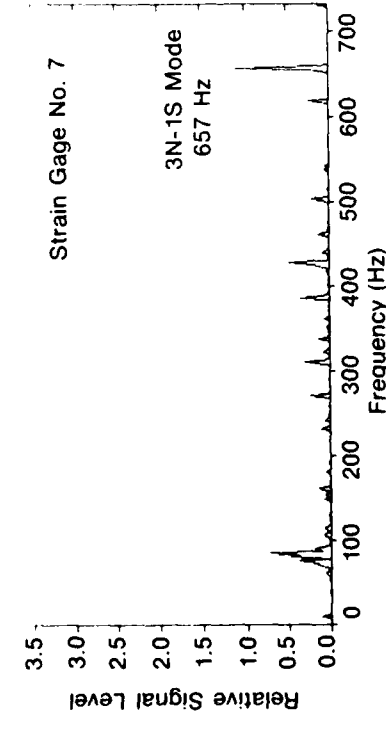
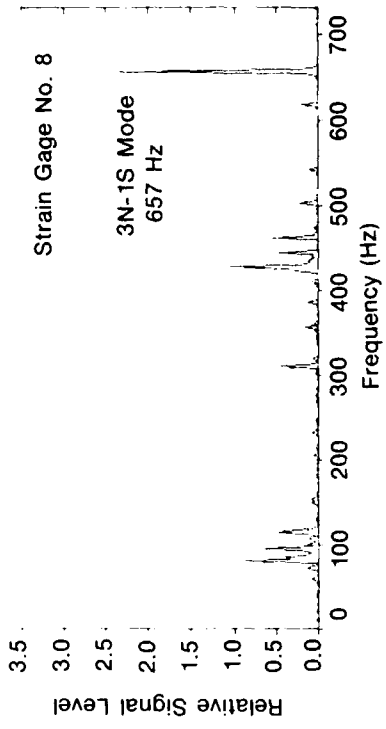
Figure 36. Spectral Response Curves for the Indicated Strain Gages Mounted on a J52 2nd-Stage Compressor Bladed-Disk Rotating at 7000 rpm and Excited in the 2N-1S Mode of Vibration With an Excitation Frequency of 334 Hz





FD 204192

Figure 37. Spectral Response Curves for the Indicated Strain Gages Mounted on a J52 2nd-Stage Compressor Bladed-Disk Rotating at 7000 rpm and Excited in the 2N-1S Mode of Vibration With an Excitation Frequency of 794 Hz



FD 204183

Figure 38. Spectral Response Curves for the Indicated Strain Gages Mounted on a J52 2nd-Stage Compressor Bladed-Disk Rotating at 7000 rpm and Excited in the 3N-1S Mode of Vibration With an Excitation Frequency of 310 Hz

## SECTION V

### CONCLUSIONS AND RECOMMENDATIONS

The objective of this program was to develop an experimental technique of image derotated holographic interferometry to investigate the resonant behavior of gas turbine engine fully bladed-disks under laboratory-controlled conditions of rotational speed and vibratory excitation. The program was intended to continue and improve the effort initiated in the feasibility study. The technique was developed during this program so that resonant modes of vibration were excited on a rotating bladed-disk with a sinusoidal force, and image derotated holograms of good quality were constructed of the resonances. The large bias fringe pattern on the holograms taken during the feasibility study was eliminated, making possible the identification and analysis of the resonant mode shapes directly from the holograms.

Although the technique has been demonstrated successfully, to become a practical analysis technique there are two areas which need improvement. First, the occurrences of the pulsed laser multimoding must be reduced in frequency to some controllable level. Secondly, although some excellent results were achieved utilizing electromagnet excitation, this excitation method has amplitude and frequency limitations which make the development of an improved excitation method desirable.

The following conclusions are a direct result of the work conducted during this program:

1. Refinements incorporated in the new spin test facility enhanced the quality of the image derotated holograms and greatly facilitated their construction
2. The ac electromagnets provided a *sinusoidal excitation of sufficient* amplitude to identify several resonant modes of vibration of the rotational bladed-disk
3. A technique was developed providing the capability of constructing image derotated holograms of the resonant response of a rotating bladed-disk.

Significant progress in the development of the image derotated holography interferometry technique in a laboratory spin test facility has been achieved during this program. To further enhance this development, it is recommended that improvements in the pulsed laser and in the excitation method be pursued. The addition of an intercavity, temperature-controlled, multielement etalon to the pulsed laser should provide the desired control over the multimoding of the laser. A program should be initiated to develop an excitation source capable of exciting a rotating blade-disk with a sinusoidal force of higher amplitude and wider frequency range than that produced by the current methods.

## REFERENCES

1. Stetson, K. A., J. N. Elkins, "Optical System for Dynamic Analysis of Rotating Structures," R77-992054, Contract F33615-75-C-2013 (March 1977).
2. Bearden, J. L., "Bladed Disk Dynamic Response," AFAPL-TR-79-2002, Contract F33615-77-C-2093 (Feb. 1979).
3. Campbell, W. E., "The Protection of Steam-Turbine Disc Wheels from Axial Vibration," presented at ASME Meeting, Cleveland, OH (May 1924).
4. MacBain, J. C., "Hologram Interferometry of Rotating Structures," Technical Digest from OSA Topical Meeting on Hologram Interferometry and Speckle Metrology, June 1980, N. Falmouth, MA.
5. Waddell, A. J., W. Kennedy, and P. Waddell, "Vibration Analysis for Static and Rotating Objects by Stroboscopic Holography," Applications of Holography, Prod. Int. Symp. Holography, Besancon, France, Paper 6-6 (July 1970).
6. Waddell, A. J., "Observation of Vibration of a Rotating Disk by Means of Stroboscopic Holography," Ph.D. Thesis, University of Strathclyde, Glasgow (1972).
7. Smith, M., "The Transverse Vibration of Stationary and Rotating Disks," Ph.D. Thesis, University of Strathclyde, Glasgow (1974).
8. Tsuruta, T., "Holographic Interferometry for Rotating Objects," Application of Holography, Proc. Int. Symp. Holography, Besancon, France, Paper 17-6 (July 1970).
9. Tsuruta, T., and Y. Itoh, "Holographic Interferometry for Rotating Subject," Applied Physics Letters, Vol. 17, No. 2 (July 1970).
10. Sikora, J. P., and F. Mendelhall, "Holographic Vibration Study of a Rotating Propeller Blade," *Experimental Mechanics*, Vol. 14, No. 6 (June 1974).
11. Sikora, J. P., H. A. Peterion, and F. T. Mendelhall, "Deflection, Stress, and Vibration Analysis of Rotating Propellers Using Holography," NSRDC Report 4507 (November 1974).
12. Waddell, P., "Strain Pattern Recognition," *Engineering Materials Design*, Vol. 17 (March 1973).
13. Waddell, P., and B. G. D. Smart, "A Non-Stroboscopic System for Examining High Speed Rotating Objects," *Strain*, Vol. 9, No. 2 (April 1973).
14. Waddell, P., "Stopping Rotary Motion with a Prism," *Machine Design*, Vol. 45, No. 12 (May 1973).
15. Waddell, P., "A Stepper Motor Controlled Image Derotator System to Non-Stroboscopically Visualize Stress, Vibration and Epicycle Motion in Real Time on High Speed Rotating Components," 4th Annual Symp. on Incremental Motion Control Systems and Devices, University of Illinois at Urbana-Champaign (April 1975).

16. Stetson, K. A., "The Use of Prime Image Derotation in Holographic Interferometry and Speckle Photography of Rotating Objects," *Experimental Mechanics*, Vol. 18, No. 2 (February 1978).
17. MacBain, J. C., J. E. Horner, W. A. Strange, and J. S. Ogg, "Vibration Analysis of a Spinning Disk Using Image-Derotated Holographic Interferometry," *Experimental Mechanics*, Vol. 19, No. 1 (January 1979).

DATE  
FILMED  
— 8